

1 *Revised MS submitted to HESS*

2 **Evaluation of Lacustrine Groundwater Discharge, Hydrologic**
3 **Partitioning, and Nutrient Budgets in a Proglacial Lake in**
4 **Qinghai-Tibet Plateau: Using ²²²Rn and Stable Isotopes**

5

6 **Xin LUO^{1,2,3}, Xingxing Kuang⁴, Jiu Jimmy Jiao^{1,2,3*}, Sihai Liang⁵, Rong Mao^{1,2,}**
7 **⁴, Xiaolang Zhang^{1,2,4}, and Hailong Li⁴**

8

9 ¹Department of Earth Sciences, The University of Hong Kong, P. R. China

10 ²The University of Hong Kong, Shenzhen Research Institute (SRI), Shenzhen, P. R.
11 China

12 ³The University of Hong Kong-Zhejiang Institute of Research and Innovation
13 (HKU-ZIRI), Hangzhou, PR China

14 ⁴School of Environmental Science and Engineering, Southern University of Science
15 and Technology, 1088 Xueyuan Rd., Shenzhen, China

16 ⁵School of Water Resources & Environment, China University of Geosciences, 29
17 Xueyuan Road, Beijing, China

18

19

20

21 Corresponding author: Jiu Jimmy Jiao (jjiao@hku.hk)

22 Department of Earth Sciences, The University of Hong Kong

23 Room 302, James Lee Science Building, Pokfulam Road, Hong Kong

24 Tel (852) 2857 8246; Fax (852) 2517 6912

25

26 **Abstract**

27 Proglacial lakes are good natural laboratories to investigate groundwater and
28 glacier dynamics under current climate condition and to explore biogeochemical
29 cycling under pristine lake status. This study conducted a series of investigations of
30 ^{222}Rn , stable isotopes, nutrients and other hydrogeochemical parameters in Ximen Co
31 Lake, a remote proglacial lake in the east of Qinghai-Tibet Plateau (QTP). A radon
32 mass balance model was used to quantify the lacustrine groundwater discharge (LGD)
33 of the lake, leading to an LGD estimate of $10.3 \pm 8.2 \text{ mm d}^{-1}$. Based on the three end
34 member models of stable ^{18}O and Cl^- , the hydrologic partitioning of the lake is
35 obtained, which shows that groundwater discharge only accounts for 7.0 % of the
36 total water input. The groundwater derived DIN and DIP loadings constitute 42.9 %
37 and 5.5 % of the total nutrient loading to the lakes, indicating the significance of LGD
38 in delivering disproportionate DIN into the lake. This study presents the first attempt
39 to evaluate the LGD and hydrologic partitioning in the glacial lake by coupling
40 radioactive and stable isotopic approaches and the findings advance the understanding
41 of nutrient budgets in the proglacial lakes of QTP. The study is also instructional in
42 revealing the hydrogeochemical processes in proglacial lakes elsewhere.

43 **Keywords:** Proglacial lake; ^{222}Rn ; lacustrine groundwater discharge; hydrologic
44 partitioning; nutrient budgets

45 **1. Introduction**

46 High altitude and latitude areas are intensively influenced by the melting of
47 glaciers due to climatic warming. Of particular importance are the proglacial areas,
48 such as proglacial lakes and moraines, because they are particularly affected by
49 climatic change induced glacier retreating and thawing of permafrost (Heckmann et
50 al., 2016; Barry, 2006; Slaymaker, 2011). The proglacial lakes are usually located close
51 to ice front of a glacier, ice cap or ice sheet, with the vicinity to the ice front
52 sometimes defined as the areas with subrecent moraines and formed by the last
53 significant glacier advances at the end of the Little Ice Age (Heckmann et al.,
54 2016; Barry, 2006; Slaymaker, 2011; Harris et al., 2009). These lakes are located in the
55 transition zones from glacial to non-glacial conditions, and can serve as natural
56 laboratories to explore hydrological processes, biogeochemical cycles and
57 geomorphic dynamics under current climatic conditions (Dimova et al.,
58 2015; Heckmann et al., 2015).

59 The Qinghai-Tibet Plateau (QTP), the third pole of the world, serves as the water
60 tower of most of the major rivers in Asian (Qiu, 2008). Unique landscapes such as endorheric
61 lakes, permafrost, glaciers, and headwater fluvial networks are developed due to the intensive
62 interaction between the atmosphere, hydrosphere, biosphere and cryosphere (Lei et al.,
63 2017; Zhang et al., 2017a; Zhang et al., 2017b; Yao et al., 2013; Yao et al., 2012). Distributed

64 mountainous glaciers and lakes are the most representative landscapes and are highly
65 sensitive to the climate changes. In the past decade, the lakes in the interior of the QTP show
66 overall expanding with respect to an overall increase of precipitation, accelerated glacier
67 melting and permafrost degradation (Zhang et al., 2013;Zhang et al., 2017b;Zhang et al.,
68 2017a;Heckmann et al., 2016;Yang et al., 2014). Some latest studies have made effects to
69 depict the hydrologic partitioning of the majority of the lakes in the QTP based on long term
70 observation of climatological parameters, and remote sensing approaches. However, so far a
71 quantitative evaluation of the water balance and hydrologic partitioning, especially the
72 groundwater component of the lakes in the QTP is limited due to the scarcity of observational
73 data. Therefore, there is a great need to conduct refined and systematical field observation to
74 provide groundtruth dataset and tenable models to depict the water balance and hydrologic
75 partitioning of the lakes, especially proglacial lakes in the QTP (Yang et al., 2014;Zhang et al.,
76 2017b).

77 Mountainous proglacial lakes, formed by glacial erosion and filled by melting
78 glaciers, are widely distributed in the Qinghai-Tibet Plateau (QTP), especially along
79 the substantial glacier retreating areas of Himalaya Mountains (MT.), Qilian MT.,
80 Tienshan MT., etc. Characterized by higher elevations, small surface areas but
81 relatively large depths, mountainous proglacial lakes in QTP lack systematic
82 field-based hydrological studies due to their remote locations and difficulty in

83 conducting field work (Yao et al., 2012;Farinotti et al., 2015;Bolch et al., 2012).

84 There has been extensive recognition of the importance of groundwater discharge
85 to various aquatic systems for decades (Dimova and Burnett, 2011;Valiela et al.,
86 1978;Johannes, 1980). Very recently, the topic of ‘lacustrine groundwater discharge
87 (LGD)’, which is comprehensively defined as groundwater exfiltration from lake
88 shore aquifers to lakes (Lewandowski et al., 2015;Rosenberry et al., 2015;Blume et al.,
89 2013;Lewandowski et al., 2013), has been introduced. LGD is analogous of in
90 submarine groundwater discharge (SGD) in coastal environments. LGD also plays a
91 vital role in lake hydrologic partitioning, which is defined as the separation of
92 groundwater discharge/exfiltration, riverine inflow, riverine outflow infiltration,
93 surface evaporation and precipitation for the hydrological cycle of the lake (Luo et al.,
94 2017;Good et al., 2015). LGD also serves as an importance component in delivering
95 solutes to lakes since groundwater is usually concentrated in nutrients, CH₄, dissolved
96 inorganic/organic carbon (DIC/DOC) and other geochemical components (Paytan et
97 al., 2015;Lecher et al., 2015;Belanger et al., 1985;Dimova et al., 2015). Nutrients and
98 carbon loading from groundwater greatly influences ratios of dissolved inorganic
99 nitrogen (DIN) to dissolved inorganic phosphate (DIP) (referred as N: P ratios
100 thereafter), ecosystem structure and the primary productivity of the lake aquatic
101 system (Nakayama and Watanabe, 2008;Belanger et al., 1985;Hagerthey and Kerfoot,

102 1998).

103 The approaches to investigate LGD include 1) direct seepage meters (Shaw and
104 Prepas, 1990;Lee, 1977), 2) geo-tracers such as radionuclides, stable ^2H and ^{18}O
105 isotopes (Gat, 1995;Kluge et al., 2007;Kraemer, 2005;Lazar et al., 2008), 3) heat and
106 temperature signatures (Liu et al., 2015;Sebok et al., 2013), 4) numerical modeling
107 (Winter, 1999;Smerdon et al., 2007;Zlotnik et al., 2009;Zlotnik et al., 2010) and 5)
108 remote sensing (Lewandowski et al., 2013;Wilson and Rocha, 2016;Anderson et al.,
109 2013). Recently, some researchers started to investigate groundwater dynamics in
110 peri- and proglacial areas, mostly based on the approaches of numerical modeling
111 (Lemieux et al., 2008b;Lemieux et al., 2008c;Andermann et al., 2012;Scheidegger
112 and Bense, 2014;Lemieux et al., 2008a). However, the quantification of groundwater
113 and surface water exchange in proglacial lakes is still challenging due to limited
114 hydrogeological data and extremely seasonal variability of aquifer permeability
115 (Dimova et al., 2015;Callegary et al., 2013;Xin et al., 2013).

116 ^{222}Rn , a naturally occurring inert gas nuclide highly concentrated in groundwater,
117 can be more applicable in fresh aquatic systems and has been widely used as a tracer
118 to quantify groundwater discharge in fresh water lakes (Luo et al., 2016;Corbett et al.,
119 1997;Dimova et al., 2015;Dimova and Burnett, 2011;Dimova et al., 2013;Kluge et al.,
120 2007;Kluge et al., 2012;Schmidt et al., 2010) and terrestrial rivers and streams

121 (Burnett et al., 2010;Cook et al., 2003;Cook et al., 2006;Batlle-Aguilar et al., 2014).
122 Of particular interest are investigations of temporal ^{222}Rn distribution in lakes, since it
123 can be used to quantify groundwater discharge and reflect the locally climatological
124 dynamics (Dimova and Burnett, 2011;Luo et al., 2016). Temporal radon variations
125 give high resolution estimates of groundwater discharge to lakes over diel cycles,
126 allowing evaluation of LGD and the associated chemical loadings. However, there has
127 been no study of radon-based groundwater discharge in mountainous proglacial lakes,
128 especially for those lakes in the QTP.

129 This study aims to investigate the groundwater surface water interactions for the
130 proglacial lake of Ximen Co, by estimating the LGD and evaluating the hydrologic
131 partitioning of the lake. LGD is estimated with ^{222}Rn mass balance model, and the
132 hydrologic partitioning of the lake is obtained with the three endmember model
133 coupling the mass balance of water, stable isotopes and Cl^- . Moreover, LGD derived
134 nutrients are estimated and the nutrient budgets of the lake are depicted. This study,
135 to our knowledge, makes the first attempt to quantify the LGD, hydrologic partition,
136 and groundwater borne nutrients of the proglacial lake in QTP and elsewhere via the
137 approach integrating multiple tracers. This study provides insights of hydrologic
138 partitioning in a typical mountainous proglacial lake under current climate condition
139 and reveals groundwater borne chemical loadings in this proglacial lake in QTP and

140 elsewhere.

141

142 **2. Methodology**

143 2.1 Site descriptions

144 The Nianbaoyeze MT., located at the eastern margin of the QTP and being the
145 easternmost part of NW-SW trending Bayan Har Shan, is situated at the main water
146 divide of the upper reaches of Yellow River and Yangtze River (Figure 1). With a peak
147 elevation of 5369 m, the mountain rises about 500-800 m above the surrounding
148 peneplain and displays typical Pleistocene glacial landscapes such as moraines,
149 U-shaped valleys and cirques (Lehmkuhl, 1998; Schlutz and Lehmkuhl,
150 2009; Wischniewski et al., 2014). The present snow line is estimated to be at an
151 elevation of 5100 m (Schlutz and Lehmkuhl, 2009). Controlled by the South Asia and
152 East Asia monsoons, the mountain has an annual precipitation of 975 mm in the
153 southern part and 582 mm in the northwestern part, with 80 % occurring during May
154 and October (Yuan et al., 2014; Zhang and Mischke, 2009). The average temperature
155 gradient is about 0.55 °C per 100 m, and the closest weather station, locating in Jiuzhi
156 town (N: 33.424614 °, E: 101.485998) at the lower plains of the mountain, recorded a
157 mean annual temperature of 0.1 °C. Snowfalls occur in nearly 10 months of the entire
158 year and there is no free-frost all year around (Böhner, 1996, 2006; Schlutz and

159 Lehmkuhl, 2009). The precipitation, daily bin-averaged wind speed and temperature
160 in Aug, 2015 were recorded to be 90 mm, 0.7 m s^{-1} and $9.5 \text{ }^{\circ}\text{C}$ from Jiuzhi weather
161 station (Figure 2). The water surface evaporation was recorded to be 1429.8 mm in
162 2015 from Jiuzhi weather station.

163 Among the numerous proglacial lakes developed in the U-shaped valleys of the
164 Nianbaoyeze MT., Ximen Co lake is located at the northern margin of the mountain
165 with an elevation of 4030 m asl, and is well studied and easily accessible (Lehmkuhl,
166 1998;Zhang and Mischke, 2009;Schlutz and Lehmkuhl, 2009;Yuan et al., 2014). The
167 lake was formed in a deep, glacially eroded basin with a catchment area of 50 km^2 ,
168 and has a mean and a maximum depth of 40 m and 63.2 m, and a surface area of 3.6
169 km^2 . The vegetation around the lake is dominated by pine meadows with dwarf shrubs,
170 rosette plants and alpine cushion (Schlutz and Lehmkuhl, 2009;Zhang and Mischke,
171 2009;Yuan et al., 2014). Mostly recharged by the glacial and snowpack melting water
172 and regional precipitation, the lake is stratified with an epilimnion depth about 4.4 m
173 in the summer time. The lake is usually covered by ice in the winter time (Zhang and
174 Mischke, 2009). The superficial layer within the U-shaped valley is characterized by
175 peat, clay and fluvial gravels with a depth about 1-3.5 m. Discontinuous and isolated
176 permafrost is present at the slope of the valley above the elevation of about 4150 m.
177 The maximum frozen depth is about 1.5 m for the seasonal frozen ground around the

178 lake. The seasonal frozen ground serves as an unconfined aquifer during the unfrozen
179 months from July to October, and groundwater discharges into the epilimnion of the
180 lake (Wang, 1997; Schlutz and Lehmkuhl, 2009; Zhang and Mischke, 2009).

181

182 2.2 Sampling and field analysis

183 The field campaign to Ximen Co Lake was conducted in August, 2015, when it is
184 warm enough to take the water samples of different origins as the studied site is
185 seasonally frozen. A ^{222}Rn continuous monitoring station was setup at the southeast
186 part of the lake, where is fairly flat for setting up our tent and monitoring system.

187 Surface water samples were collected around the lake, rivers at the upstream and
188 downstream. Porewater samples were collected at one side of the lake as the other
189 side is steep and rocky. The basic water quality parameters of conductivity (EC),
190 dissolved oxygen (DO), TDS, ORP, and pH in the water were recorded with the
191 multi-parameter meter (HANNA, Co.). Relative humidity was recorded with a
192 portable thermo-hydrometer (KTH-2, Co.). Lake water samples were taken with a
193 peristaltic pump into 2.5 L glass bottles for ^{222}Rn measurement with the Big Bottle
194 system (DurrIDGE, Co.). Surface water samples were filtered with 0.45 μm filters
195 (Advantec, Co.) in situ and taken into 5 ml, 15 ml, 15 ml and 50 ml Nalgene
196 centrifugation tubes for stable isotope, major anion, cation and nutrient analysis.

197 Porewater samples were taken from the lakes shore aquifers with a push point sampler
198 (M.H.E, Co.) connected to peristaltic pump (Solinst, Co.) (Luo et al., 2014;Luo et al.,
199 2016). 100 ml raw surface water or porewater was titrated with 0.1 μM H_2SO_4
200 cartridge (Hach, Co.) in situ to measure total alkalinity (Hasler et al., 2016;White et
201 al., 2016;Warner et al., 2013). Porewater was filtered with 0.45 μm syringe filters in
202 situ and taken into 5 ml, 15 ml, 15 ml and 50 ml Nalgene centrifugation tubes for
203 stable isotope, major anion, cation and nutrient analysis. 250 ml porewater was taken
204 for ^{222}Rn measurement with RAD7 H_2O (DurrIDGE, Co.). Samples for major cation
205 analysis were acidified with distilled HNO_3 immediately after the sampling.

206 ^{222}Rn continuous monitoring station was set up at the northwest of the lake, close
207 to the downstream of the lake (Figure 1b). Lake water (about 0.5 m in depth) was
208 pumped with a DC pump (12 V) driven by lithium batteries (100 Ah) and sprinkled
209 into the chamber of RAD7 AQUA with a flow rate $> 2 \text{ L min}^{-1}$, where ^{222}Rn in water
210 vapor was equilibrated with the air ^{222}Rn . The vapor in the chamber was delivered
211 into two large dry units (Drierite, Co) to remove the moisture and circulated into
212 RAD7 monitor, where ^{222}Rn activities were recorded every 5 mins. A temperature
213 probe (HOBO[®]) was insert into the chamber to record the temperature of the water
214 vapor. The monitoring was performed from 11: 31 am, Aug 22nd to 6: 30 am, Aug 24th,
215 2015. During the period of 1:50-4:30 pm on Aug 22nd, a sudden blizzard occurred,

216 leading to an hourly precipitation about 0.6 mm to the lake area. Daily and hourly
217 climatological data such as wind speed, air temperature and precipitation were
218 retrieved from the nearest weather station in Jiuzhi town (N: 33.424614 °, E:
219 101.485998). Moreover, another RAD7 was placed at the lakes hore to measure ^{222}Rn
220 in the ambient air around the lake. Due to extremely low activities, the monitoring
221 period was conducted only for 4 hours, and the mean activity was adopted as the
222 background radon-222 activity to be used in the mass balance model. Water level and
223 temperature fluctuations were recorded with a conductivity-temperature-depth diver
224 (Schlumberger, Co.) fixed at about 20 cm below the lake surface and calibrated with
225 local atmospheric pressure recorded by a baro-diver (Schlumberger, Co.) above the
226 lake. To correct for dissolved ^{226}Ra supported ^{222}Rn , one radium sample was extracted
227 from 100 L lake water with MnO_2 fiber as described elsewhere (Luo et al.,
228 2014;Moore, 1976).

229

230 2.3 Chemical analysis

231 Major ions were measured with ICS-1100 (Dionex. Co.) in the Department of Earth
232 Sciences, the University of Hong Kong. The uncertainties of the measurements are
233 less than 5 %. Nutrients, DIN and DIP were analyzed with flow injection analysis
234 equipped with auto-sampler (Lachat. Co.) in the School of Biological Sciences, the

235 University of Hong Kong. Stable ^{18}O and ^2H isotopes were measured with
236 MOA-ICOS laser absorption spectrometer (Los Gatos Research (LGR) Triple Isotope
237 Water Analyzer (TIWA-45EP)) at State Key Laboratory of Marine Geology, Tongji
238 University, Shanghai. The stable isotopic standards and the recovery test have been
239 fully described elsewhere (Luo et al., 2017). The measurement uncertainty is better
240 than 0.1 % for ^{18}O and 0.5 % for ^2H . ^{226}Ra was detected with RAD7 with the method
241 described elsewhere (Kim et al., 2001; Lee et al., 2012; Luo et al., 2018).

242

243 2.4 Radon transient model

244 Previous studies employed a steady state radon-222 mass balance model to
245 quantify LGD to lentic system such as lakes and wetlands (Dimova and Burnett,
246 2011; Luo et al., 2016). This model assumes that radon input derived from
247 groundwater inflow, diffusion and river inflow are balanced by the radon losses of
248 atmospheric evasion, decay and river outflow. However, recent studies revealed that
249 the steady state is mainly reached after 2-15 days of constant metrological conditions,
250 and most lentic system cannot be treated as steady state due to rapid radon-222
251 degassing to the atmosphere driven by wind-induced turbulence (Gilfedder et al.,
252 2015; Dimova and Burnett, 2011).

253 Ximen Co lake is demonstrated to be highly stratified with an epilimnion of 4.4

254 m (Zhang and Mischke, 2009). The lake was formed by glacier erosion and the
 255 lakebed is characterized by granite bedrock with a thin sedimentary clay layer.
 256 Previous studies have indicated that sediment consisting of clay, soils and gravels has
 257 been developed on the bedrock and forms the lake shore aquifer with a thickness of
 258 0.7-3.3 m (Schlutz and Lehmkühl 2009). Porewater sampled in the aquifer immediate
 259 behind the lake shore can well represent groundwater discharging into the lake, as
 260 suggested previously (Lewandowski et al., 2015; Rosenberry et al., 2015; Schafran and
 261 Driscoll, 1993). LGD has been widely considered to occur within the first few meters
 262 of the lake shore (Schafran and Driscoll, 1993; Rosenberry et al., 2015; Lee et al., 1980)
 263 and groundwater is considered to predominately discharge into the epilimnion since
 264 deep groundwater flow is highly limited by the Precambrian bedrock (Einarsdottir et
 265 al., 2017). Due to negligible hydrological connection between the epilimnion and
 266 hypolimnion, ²²²Rn mass balance model is established to quantify LGD to the
 267 epilimnion from the lake shore.

268 The governing equation of radon-222 transient mass balance model within a 1 x
 269 1 x z cm (where z is the depth in cm) can be expressed as (Gilfedder et al., 2015):

$$270 \quad z \frac{\partial I_w}{\partial t} = F_{gw} + (I_{^{226}Ra} - I_w) \times z \times \lambda_{222} + F_{diff} - F_{atm} \quad (1)$$

271 where F_{gw} , F_{diff} , F_{atm} [$Bq \ m^{-2} \ d^{-1}$] are ²²²Rn loadings from LGD, water-sediment
 272 diffusion and water-air evasion, respectively; z [m] is the lake water level depth

273 recorded by the diver. λ_{222} is the decay constant of ^{222}Rn with a value of 0.186 d^{-1} .
274 $\lambda_{222} \times I_{^{226}\text{Ra}}$ and $\lambda_{222} \times I_w$ account for the production and decay of ^{222}Rn [$\text{Bq m}^{-2} \text{ d}^{-1}$]
275 in the water column, respectively. I_w and $I_{^{226}\text{Ra}}$ [Bq m^{-2}] represent ^{222}Rn and ^{226}Ra
276 inventories in the epilimnion, and are expressed as: $I_w = H \times C_w$ and
277 $I_{^{226}\text{Ra}} = H \times C_{^{226}\text{Ra}}$, respectively; where H [m] is the depth of the epilimnion; C_w and
278 $C_{^{226}\text{Ra}}$ is the ^{222}Rn and ^{226}Ra activity [Bq m^{-3}], respectively.

279 The model is valid under the following assumptions: 1) The epilimnion is well
280 mixed which is the actual condition for most natural boreal and high altitude glacial
281 lakes (Zhang and Mischke, 2009; Åberg et al., 2010). 2) ^{222}Rn input from riverine
282 water inflow, and loss from the lake water outflow and infiltration into the lake shore
283 aquifer is negligible compared to the groundwater borne ^{222}Rn , because ^{222}Rn
284 concentration of groundwater is 2-3 orders of magnitude larger than that of lake water
285 (Dimova and Burnett, 2011; Dimova et al., 2013). Generally, ^{222}Rn in the epilimnion is
286 sourced from LGD and decay input from parent isotope of ^{226}Ra under secular
287 equilibrium, and is mainly lost via atmospheric evasion and radioactive decay.

288 F_{atm} is the key sinking component of the transient model and is finally a function of
289 wind speed and water temperature, both of which are temporal variant variables
290 (Supplementary information). Lake water level z is also a temporal variant variable
291 which represents the fluctuations of water volume of the epilimnion. This equation is

292 discretized by the forward finite difference method, and the groundwater flux at each
293 time step can be solved as follow

294
$$[{}^{222}\text{Rn}_{t+\Delta t}] = \frac{[z \times {}^{222}\text{Rn}_t + [F_{diff} + F_{gw} - F_{atm} - {}^{222}\text{Rn}_t \times \lambda \times z] \times \Delta t}{z} \quad (2)$$

295 where ${}^{222}\text{Rn}_{t+\Delta t}$ and ${}^{222}\text{Rn}_t$ [Bq m⁻³] is the ²²²Rn activity at current time step and at
296 the previous time steps, respectively, and Δt [min] is the time step which is set to be
297 5 min in consistence with the ²²²Rn record interval. With the inverse calculation based
298 on Equation (2), the groundwater inflow at each time step can be obtained. However,
299 large errors of the final LGD calculation will be induced by even a small amount of
300 noise in the measured ²²²Rn data due to the ${}^{222}\text{Rn}_{t+\Delta t} - {}^{222}\text{Rn}_t$ term being with the
301 measure uncertainty. To reduce the random errors of the measured ²²²Rn
302 concentrations, the time window with a width of 1 hour is proposed to smooth the
303 curve (Supplementary information).

304

305 3. Results

306 3.1 Time series data

307 Figure 2 shows the basic climatological parameters of the lake catchment during
308 the campaign month. There are discrete rainfall events occurring throughout the
309 month with an average rainfall of 3.1 mm d⁻¹. The temperature during the month
310 ranges from 5.0 – 12.5 °C within an average of 9.3 °C. The daily averaged wind speed
311 ranges from 0.7 – 2.5 m s⁻¹, with an average of 1.7 m s⁻¹. ²²²Rn temporal distribution

312 and other time series data are shown in Figure 3a and listed in Supplementary Table 1.
313 Generally, ^{222}Rn concentration varies from 32.2 to 273 Bq m^{-3} , with an average of
314 $144.2 \pm 27.7 \text{ Bq m}^{-3}$. ^{222}Rn over the monitoring period shows typical diel cycle, much
315 higher at nighttime and lower in the day time. Figures 3b-3d show the time series data
316 of temperature (5 mins interval), nearshore lake water level (1 min interval), and wind
317 speed (1 hour interval). Temperature and lake water level also show typical diel cycles,
318 but with antiphase fluctuations with each other. Temperature is higher during the
319 daytime and lower at nighttime. However a sudden decrease of temperature was
320 recorded due to the sudden blizzard (Figure 3b). Water level is higher at nighttime and
321 lower during the daytime, with a strong fluctuation due to the turbulence caused by
322 the blizzard (Figure 3c). The variability might reflect the dynamics of groundwater
323 input and surface water inflow. The air temperature of the lake area is in phase with
324 the water temperature. Wind speed is normally higher during the daytime and lower at
325 nighttime (Figure 3d).

326 The variation of ^{222}Rn is nearly in antiphase with the fluctuations of lake water
327 temperature and air temperature, indicating that the dominated controlling factors of
328 ^{222}Rn fluctuations are water temperature and wind speed (Figure 3a). This
329 phenomenon is reasonable as lake water ^{222}Rn is predominately lost via atmospheric
330 evasion, which is the function of wind speed and water temperature (Dimova et al.,

331 2015;Dimova and Burnett, 2011;Dimova et al., 2013). High water temperature and
332 wind speed leads to elevated atmospheric evasion and causes the decline of ^{222}Rn
333 concentration in the lake water. However, there is a sudden reduction of radon activity
334 from 2: 00 pm to 4: 00 pm on Jul 22nd, 2015, when the snow event led to a sudden
335 decrease of water temperature, increase of wind speed, and large surface water
336 turbulence as indicated by water level fluctuations (Figures 3a-3d). ^{222}Rn in the
337 porewater is 2-3 orders of magnitude larger than ^{222}Rn in the lake water, suggesting
338 that ^{222}Rn is an ideal tracer to estimate the LGD (Supplementary Table 1). ^{222}Rn
339 concentrations in surface water range from 22.2 to 209 Bq m⁻³, with an average of
340 92.5 Bq m⁻³ (n = 12), which is in the range of ^{222}Rn continuous monitoring results,
341 suggesting reliable ^{222}Rn measurements (Supplementary Table 2).

342

343 3.2 Geochemical results

344 The results of major ions, nutrients and stable isotopes in different water
345 endmembers are shown in Figures 4 and 5. Cl^- ranges from 0.6 to 2.1 mg L⁻¹ in the
346 surface water (including riverine inflow water, lake water and downstream water), 0.4
347 to 2.7 mg L⁻¹ in porewater and has a much higher concentration of 5.9 mg L⁻¹ in
348 rainfall water. Na^+ ranges from 1.6 to 3.4 mg L⁻¹ in the surface water, 1.2 to 4.4 mg
349 L⁻¹ in porewater and has a concentration of 4.4 mg L⁻¹ in rainfall water. SO_4^{2-} ranges

350 from 1.2 to 2.3 mg L⁻¹ in the surface water, 0.4 to 1.7 mg L⁻¹ in porewater and has a
351 significant low concentration of 0.01 mg L⁻¹ in rainfall water. Ca²⁺ ranges from 3.0 to
352 12.4 mg L⁻¹ in lake water, 3.4 to 12.5 mg L⁻¹ in porewater and has a significantly high
353 concentration of 20.5 mg L⁻¹ in rainfall water. Other concentrations of major ions are
354 listed in Supplementary Table 2. As shown in Figure 4d and Supplementary Table 2,
355 $\delta^{18}\text{O}$ in the lake water ranges from - 13.06 ‰ to - 12.11 ‰, with an average of -
356 12.41 ‰ (n = 7), and $\delta^2\text{H}$ ranges from - 91.83 ‰ to - 87.47 ‰, with an average of -
357 89.0 ‰ (n = 7). $\delta^{18}\text{O}$ in the riverine inflow water ranges from - 13.44 ‰ to - 13.29 ‰,
358 with an average of - 13.37 ‰ (n = 2), and $\delta^2\text{H}$ ranges from - 93.25 ‰ to - 91.92 ‰,
359 with an average of - 92.59 ‰ (n = 2). $\delta^{18}\text{O}$ in the downstream water ranges from -
360 12.51 ‰ to - 12.18 ‰, with an average of - 12.35 ‰ (n = 3), and $\delta^2\text{H}$ ranges from -
361 88.96 ‰ to - 87.1 ‰, with an average of - 87.98 ‰ (n = 3). $\delta^{18}\text{O}$ in the porewater
362 ranges from - 12.66 ‰ to - 11.52 ‰, with an average of - 11.97 ‰ (n = 8), and $\delta^2\text{H}$
363 ranges from - 91.3 ‰ to - 82.87 ‰, with an average of - 85.5 ‰ (n = 8). DIN in the
364 surface water (including riverine inflow water, lake water and downstream water)
365 ranges from 6.6 to 16.9 μM , with an average of 10.3 μM , and DIP from 0.36 to 0.41
366 μM , with an average of 0.38 μM . DIN for the porewater ranges from 0.7 to 358.8 μM ,
367 with an average of 92.8 μM , and DIP from 0.18 to 0.44 μM with an average of 0.31
368 μM (Figure 5).

369

370 **4. Discussion**

371 4.1 Proglacial hydrologic processes and geochemical implications

372 Generally, major ion concentrations in the lake water and porewater of Ximen
373 Co lake are significantly lower than those in major rivers, streams and other tectonic
374 lakes in the QTP (Yao et al., 2015;Wang et al., 2010;Wang et al., 2016b), and are
375 similar to those of snow and glaciers (Liu et al., 2011), suggesting that the lake water
376 is mainly originated from glacier and snow melting. Ion concentrations in the lake and
377 porewater of Ximen Co lake are much lower than those of rainfall collected in Jiuzhi
378 town. This suggests that lake water is less influenced by precipitation (Figures 4a-4c).
379 The concentrations of major ions in the porewater are high compared to the lake water,
380 indicating weathering affects from the aquifer grains. The ratios of $\text{Ca}^{2+}/\text{Na}^{+}$ in the
381 porewater and groundwater is >1 , also suggesting influences of weathering diagenesis
382 of major ions from the seasonal frozen ground at the lake shore aquifer (Weynell et al.,
383 2016;Yao et al., 2015;Wang et al., 2010).

384 The isotopic compositions of the lake water and porewater are significantly
385 isotopically depleted, with values close to the compositions of glaciers and surface
386 snow in the QTP, suggesting the lake is dominantly recharged from snow and glacier
387 melting (Cui et al., 2014;Wang et al., 2016a;Zongxing et al., 2015). The relation of

388 $\delta^{18}\text{O}$ versus $\delta^2\text{H}$ for the lake water is $\delta^2\text{H} = 4.25 \times \delta^{18}\text{O} - 35.99$, with a slope much
389 lower than that of the global meteoric water line (GMWL) (Figure 4d), suggesting the
390 effects of lake surface evaporation. The relation of $\delta^{18}\text{O}$ versus $\delta^2\text{H}$ for the porewater
391 is $\delta^2\text{H} = 6.93 \times \delta^{18}\text{O} - 2.67$, overall on GWML (Figure 4d). Deuterium excesses is
392 defined as $\Delta\text{D} = \delta\text{D} - 8 \times \delta^{18}\text{O}$ (Dansgaard, 1964). The value of ΔD is dependent on
393 air mass origins, altitude effect and the kinetic effects during evaporation (Hren et al.,
394 2009). Global meteoric water has a ΔD of + 10 ‰. In the QTP, glacier/snowpack
395 melting water usually has large positive ΔD , while the precipitations derived from
396 warm and humid summer monsoon has lower ΔD (Ren et al., 2017; Ren et al., 2013).
397 In this study, ΔD of surface water, lake and porewater ranges from + 8.5 to + 11.8 ‰,
398 closed to the glacier melting water but much smaller than that of the local
399 precipitation of + 18.8 ‰. This indicates the stream and lake water are mainly
400 originated from glacial/snowpack melting rather than precipitation (Gat, 1996; Wang
401 et al., 2016a; Lerman et al., 1995). The slopes of $\delta^2\text{H}$ versus $\delta^{18}\text{O}$ in lake water and
402 porewater are 4.25 and 6.93, both of which are lower than that of GMWL due to
403 surface evaporation. Lake water is more intensively influenced by evaporation
404 compared to porewater. The plots of $\delta^{18}\text{O}$ versus Cl^- , and $\delta^2\text{H}$ versus Cl^- are well
405 clustered for porewater end member (orange area), lake water end member (blue area),
406 riverine inflow water end member (yellow area), and precipitation water (Figures 4e

407 and 4f), suggesting stable $\delta^{18}\text{O}$ and $\delta^2\text{H}$ isotopes and Cl^- can serve as tracers to
408 quantify the hydrologic partitioning of the lake by setting three endmember models.

409 The concentrations of DIN and DIP are all within the ranges of other glacial
410 melting water and proglacial lake water (Hawkings et al., 2016;Hodson, 2007;Hudson
411 et al., 2000;Tockner et al., 2002;Hodson et al., 2005). Briefly, rainfall and upstream
412 lake water such as YN-4 have the highest DIN concentrations, indicating the glacier
413 melting and precipitation could be important DIN sources in proglacial areas
414 (Dubnick et al., 2017;Anderson et al., 2017). DIN in porewater is overall higher
415 compared to the lake water, suggesting the porewater to be DIN effective source; and
416 DIP concentration is higher in the lake water compared to porewater, suggesting the
417 porewater is a DIP sink (Figure 5). The N: P ratios in the lake water and porewater are
418 averaged to be 27.1 and 320.5, respectively, both much larger than the Redfield Ratio
419 (N: P = 16:1) in water and organism in most aquatic system and within the range of
420 other proglacial lakes (Anderson et al., 2017). This also suggests that the lake water
421 and porewater are under phosphate limited condition. N: P ratio in the rainfall water is
422 30.4, similar to the lake water. The average N: P ratio of porewater is much higher
423 than that of lake water, indicating DIN enrichment in the lake shore aquifers (Figure
424 5). In pristine groundwater, NO_3^- is the predominated form of dissolved nitrogen and
425 is highly mobile within the oxic aquifers, leading to much higher DIN concentrations

426 in the porewater; DIP has high affinity to the aquifer grains, resulting in much lower
427 DIP concentrations in the porewater (Lewandowski et al., 2015; Rosenberry et al.,
428 2015; Slomp and Van Cappellen, 2004). Thus, in analogous to surface runoff from
429 glacier/snowpack melting, LGD can be also regarded as an important DIN source for
430 the proglacial lakes. Because of very high DIN and N: P ratios in the porewater, a
431 relatively small portion of LGD delivers considerable nutrients into the glacial lake,
432 shifting the aquatic N: P ratios and affecting the proglacial aquatic ecosystem
433 (Anderson et al., 2017).

434

435 4.2 Estimation of LGD

436 Figure 6a shows all the sinks and sources of radon with the epilimnion of the lake.
437 Within ^{222}Rn transient mass balance model, the dominant ^{222}Rn loss is atmospheric
438 degassing/evasion. Generally, ^{222}Rn degassing rate is the function of the radon-222
439 concentration gradient at the water-air interface and the parameter of gas piston
440 velocity k , which is finally the function of wind speed and water temperature (Dimova
441 and Burnett, 2011; Gilfedder et al., 2015). To evaluate ^{222}Rn evasion rate, this study
442 employs the widely used method proposed by MacIntyre et al. (1995) which is also
443 detailed described in supplementary information. Based on the field data of ^{222}Rn
444 concentration in the lake water, wind speed and temperature log, the radon degassing

445 rate is calculated in a range of 0.8 to 265.2 Bq m² d⁻¹, with an average 42.0 of Bq m²
446 d⁻¹.

447 In addition to the atmospheric loss and sedimentary diffusion inputs, ²²²Rn is also
448 sinked via radioactive decay, and sourced from decay of parent isotope of ²²⁶Ra. The
449 decay loss of ²²²Rn fluctuates in phase with the distribution of ²²²Rn concentration
450 monitored by RAD 7 AQUA. The equations to estimate benthic fluxes are shown in
451 supplementary information. The decay loss is calculated to be 26.4 to 223.4 Bq m⁻² d⁻¹,
452 with an average of 118.0 ± 22.7 Bq m⁻² d⁻¹. ²²⁶Ra concentration is 0.01 Bq m⁻³ for the
453 lake water. Under secular equilibrium, the ²²⁶Ra decay input can be calculated by
454 multiplying ²²⁶Ra concentration in the lake water with λ_{222} (Corbett et al., 1997; Kluge
455 et al., 2007; Luo et al., 2016). ²²⁶Ra decay input is calculated to be 0.83 Bq m⁻² d⁻¹,
456 which is significantly low compared to other ²²²Rn sources to the epilimnion.

457 With the obtained sinks and sources of ²²²Rn in the lake, and the constants given in
458 Table 1, LGD rate can be obtained by dividing the groundwater derived ²²²Rn with its
459 concentration in groundwater endmember. The obtained LGD rate, ranges from -23.7
460 mm d⁻¹ to 90.0 mm d⁻¹, with an average of 10.3 ± 8.2 mm d⁻¹ (Figure 7). The LGD
461 rate range is relatively smaller than the daily lake water level variations (≈ 50 mm),
462 indicating that the lake water level variation could be a combined effect of surface
463 runoff and LGD (Hood et al., 2006). The negative values of LGD rate reflect the

464 return groundwater flow due to infiltration into the porewater. Normally, the
465 dominant values are positive, indicating LGD rate is significant compared to water
466 infiltration into lake shore aquifer. The temporal variation of LGD rate could be
467 attributed to the fluctuations of the hydraulic gradient in the proglacial areas (Hood et
468 al., 2006;Levy et al., 2015). As indicated by ΔD (mostly > 10) of surface water, the
469 lake and the upstream water is considered to be mainly recharged from
470 glacial/snowpack melting rather other precipitations.

471 To assess the magnitude of uncertainty of ^{222}Rn transient model, the sensitivity of
472 estimated LGD to changes in other variables is examined. A sensitivity coefficient f is
473 proposed to evaluate this uncertainty according to Langston et al. (2013)

$$474 \quad f = (\Delta F_{LGD} / F_{LGD}) / (\Delta y_i / y_i) \quad (3)$$

475 where ΔF_{LGD} is the amount of change in F_{LGD} from the original value. Δy_i is the
476 amount of change in the other variable of y_i from the original value. Thus, higher f
477 indicates a large uncertainty of final LGD estimate. The uncertainty mainly stems
478 from ^{222}Rn measurements in different water endmembers, the atmospheric loss and
479 water level record. The uncertainties of ^{222}Rn measurement are about 10 % and 15-20
480 % in groundwater and lake water endmember, respectively. The uncertainty of
481 atmospheric loss is derived from uncertainty of ^{222}Rn in lake water (with an
482 uncertainty of 15-20 %), temperature (with an uncertainty ≈ 5 %) and wind speed

483 (with an uncertainty $\approx 5\%$). Thus, the final LGD estimate has an integrated
484 uncertainty of 35-40 %.

485

486 **4.3 Hydrologic partitioning**

487 Compared to the groundwater labeled radionuclide of ^{222}Rn , stable $^{18}\text{O}/^2\text{H}$
488 isotopes are advantageous in the investigation of evaporation processes due to their
489 fractionations from water to vapor and have been widely used to investigate the
490 hydrologic cycle of lakes in various environments (Stets et al., 2010; Gat,
491 1995; Gonfiantini, 1986; Gibson et al., 1993). With the field data of stable isotopic
492 composition and Cl^- concentrations in different water endmembers, groundwater input,
493 surface water input, lake water outflow and infiltration, and evaporation can be
494 partitioned by coupling stable isotopic mass balance model with Cl^- mass balance
495 model (Figure 6b).

496 The model, consisting of the budgets of stable isotopes and Cl^- , and water masses
497 for the epilimnion, is used to quantify riverine inflow, lake water outflow and
498 infiltration, and evaporation (LaBaugh et al., 1995; LaBaugh et al., 1997; Gibson et al.,
499 2016). The model is valid under the following assumptions: (1) constant density of
500 water; (2) no long-term storage change in the reservoir; (3) well-mixed for the
501 epilimnion (Gibson, 2002; Gibson et al., 2016; Gibson and Edwards, 2002; LaBaugh et

502 al., 1997). The above assumptions are reasonably tenable during the short monitoring
 503 period. The model can be fully expressed as

504
$$F_{in} + F_{LGD} + F_p = F_E + F_{out} \quad (4)$$

505
$$F_{in} \times \delta_{in} + F_{LGD} \times \delta_{gw} + F_p \times \delta_p = F_E \times \delta_E + F_{out} \times \delta_L \quad (5)$$

506
$$F_{in} \times [Cl^-]_{in} + F_{LGD} \times [Cl^-]_{gw} + F_p \times [Cl^-]_p = F_E \times [Cl^-]_L + F_{out} \times [Cl^-]_{out} \quad (6)$$

507 where F_{in} [mm d⁻¹] is the surface water inflow to the lake; F_{gw} [mm d⁻¹] is LGD rate.
 508 F_p [mm d⁻¹] is the mean daily rainfall rate during the sampling period. F_E [mm d⁻¹] is
 509 the lake evaporation. F_{out} [mm d⁻¹] is the lake water outflow via runoff and
 510 infiltration into the lake shore aquifer. δ_{in} , δ_{gw} , δ_E and δ_p are the isotopic compositions
 511 of surface water inflow, LGD, and evaporative flux, respectively. The values of δ_{in} ,
 512 δ_{gw} , and δ_p are obtained from field data and the composition of δ_E are calculated as
 513 shown in supplementary information. $[Cl^-]_{in}$, $[Cl^-]_{gw}$, $[Cl^-]_L$ and $[Cl^-]_p$ are the
 514 chloride concentrations in the inflow water, porewater, lake water and precipitation,
 515 respectively.

516 The components of the mass balance model can be obtained from the field data of
 517 isotopic composition and Cl⁻ concentrations in different water endmembers. The
 518 average ¹⁸O composition -13.37 ‰ of riverine inflow water is taken as the value of
 519 the input parameter δ_{in} . $\delta^{18}O$ and δ^2H in the groundwater endmember and lake water
 520 end member are calculated to be -12.41 ‰ and -87.18 ‰, respectively. $\delta^{18}O$ and δ^2H

521 in the rainfall are measured to be -5.47 ‰ and -24.98 ‰, respectively. With the
522 measured values of δ_L , h , δ_{in} , and the estimated ε and δ_a , the isotopic composition
523 of δ_E is calculated to be -35.11 ‰, which is in line with the results of alpine and
524 arctic lakes elsewhere (Gibson, 2002;Gibson et al., 2016;Gibson and Edwards, 2002).
525 The values of $[Cl^-]_{in}$, $[Cl^-]_{gw}$, and $[Cl^-]_L$ are calculated to be 0.91 mg L⁻¹, 1.48
526 mg L⁻¹ and 1.02 mg L⁻¹, respectively. All the parameters used in the model are shown
527 in Table 2.

528 According to Equations 4-6, the uncertainties of calculations of F_{in} , F_{out} and E are
529 mainly derived from the uncertainty of F_{LGD} and the compositions of Cl⁻, δD and $\delta^{18}O$
530 in different water endmembers as suggested in previous studies (Genereux,
531 1998;Klaus and McDonnell, 2013). The compositions of Cl⁻, δD and $\delta^{18}O$ in surface
532 water, groundwater endmembers have an uncertainty of 5 %. The uncertainty of δ_E is
533 reasonably assumed to be ≈ 20 % . Thus, considering the uncertainty propagation of
534 all the above parameters, the uncertainties of F_{in} , F_{out} and E would be scaled up to
535 70-80 % of the final estimates.

536

537 4.4 The hydrologic partitioning of the glacial lake

538 Based on the three endmember model of ^{18}O and Cl⁻, the riverine inflow rate was
539 calculated to be 135.6 ± 119.0 mm d⁻¹, and the lake outflow rate is estimated to be

540 $141.5 \pm 132.4 \text{ mm d}^{-1}$; the evaporation rate is calculated to be $5.2 \pm 4.7 \text{ mm d}^{-1}$. The
541 summary of the hydrologic partitioning of the lake is shown in Figure 8a. Generally,
542 the proglacial lake is mostly recharged by the riverine inflow from the snowpack or
543 the glacier melting. The groundwater discharge contributes about only 7.0 % of the
544 total water input to the lake, indicating groundwater input does not dominate water
545 input to the proglacial lake. The recent review on LGD rate by Rosenberry et al.
546 (2015) suggests that the median of LGD rate in the literatures is 7.4 mm d^{-1} (0.05 mm
547 d^{-1} to 133 mm d^{-1}), which is about 2/3 of LGD rate in this study. This difference may
548 be due to the hydrogeological setting of the lake shore aquifer. This aquifer is formed
549 by grey loam, clayey soil and sand (Lehmkuhl, 1998; Schlutz and Lehmkuhl, 2009),
550 which is with relatively high permeability.

551 Previous studies have indicated that groundwater forms a key component of
552 proglacial hydrology (Levy et al., 2015). However, there have been limited
553 quantitative studies of groundwater contribution to hydrologic budget of proglacial
554 areas. This study further summarizes the groundwater discharge studies over the
555 glacial forefield areas. Based on long term hydrological and climatological parameter
556 monitoring on the Nam Co lake in the QTP, Zhou et al. (2013) estimated the LGD to
557 be $5\text{-}8 \text{ mm d}^{-1}$, which is comparable to the surface runoff input and LGD of this study.
558 Brown et al. (2006) investigated the headwater streams at the proglacial areas of

559 Taillon Glacier in French and found that groundwater contributes 6-10 % of the
560 stream water immediate downwards of the glacier. Using water mass balance model,
561 Hood et al. (2006) shows that groundwater inflow is substantial in the hydrologic
562 partitioning of the proglacial Lake O'Hara in front of Opabin Glacier in Canada and
563 comprised of 30 -74 % of the total inflow. Roy and Hayashi (2008) studied the
564 proglacial lakes of Hungabee lake and Opabin lake at glacier forefield of Opabin
565 Glacier and found that groundwater component is predominant water sources of the
566 lakes and consisted of 35-39 % of the total water input of the lakes. Langston et al.
567 (2013) further investigated a tarn immediate in front of Opabin Glacier and indicated
568 the tarn is predominantly controlled by groundwater inflow/outflow, which consisted
569 of 50-100 % of total tarn volume. Magnusson et al. (2014) studied the streams in the
570 glacier forefield of Dammagletscher, Switzerland and revealed that groundwater
571 contributed only 1-8 % of the total surface runoff. Groundwater contribution in this
572 study is similar to those obtained the mountainous proglacial areas in Europe, but
573 much lower than those obtained in the proglacial areas of polar regions. It is
574 concluded that proglacial lakes/streams in front of mountainous glaciers are mainly
575 recharged by surface runoff from glacier/snowpack melting. This might be due to
576 well-developed stream networks and limited deep groundwater flow (Einarsdottir et
577 al., 2017;Brown et al., 2006;Magnusson et al., 2014). However, proglacial tarns and

578 lakes in the polar areas are predominantly controlled by groundwater discharge, due
579 to less connectivity of surface runoff and high shallow and deep groundwater
580 connectivity (Langston et al., 2013; Hood et al., 2006; Roy and Hayashi, 2008).

581 The evaporation constitutes relatively small ratio ($\approx 3.5\%$) of total water losses. The
582 annual evaporation rate was recorded to be 1429.8 mm (equivalent to 3.92 mm d^{-1}) in
583 2015 by the Jiuzhi weather station, lower than the obtained evaporation in this study.
584 This may be due to much higher evaporation in August during the monitoring period.

585 The estimation of evaporation in this study generally represents the upper limit of the
586 lake, as the sampling campaign was conducted during the summer time when the
587 highest evaporation might occur. The lake surface evaporation derived from the pan
588 evaporation in the QTP ranges from $\sim 700\text{ mm yr}^{-1}$ in the eastern QTP to over 1400
589 mm yr^{-1} in the interior lakes of the QTP (Zhang et al., 2007; Ma et al., 2015; Yang et
590 al., 2014). The evaporation of this study is rather in line with the previous evaporation
591 observation in the eastern QTP, stressing the tenability of evaporation in this study.

592 The runoff input is predominated recharge component ($> 90\%$) compared to other
593 components, with an area normalized value comparable to previous studies of runoff
594 input in other glacial melting dominant lakes in the QTP (Zhou et al., 2013; Zhang et
595 al., 2011; Biskop et al., 2016). The runoff input and the lake evaporation of the study
596 area, however, are subject to highly daily, seasonal and inter-annual variability as

597 indicated by previous studies in the QTP (Zhou et al., 2013;Lei et al., 2017;Ma et al.,
598 2015;Lazhu et al., 2016). Therefore, further investigations of long term and high
599 resolution climatological and isotopic data are required to provide precise constraints
600 of hydrologic partitioning of the lakes in the QTP.

601 4.5 LGD derived nutrient loadings, nutrient budget and ecological implications

602 Compared to extensive studies of SGD derived nutrient loadings in the past decade
603 (Luo and Jiao, 2016;Slomp and Van Cappellen, 2004), studies of LGD derived
604 nutrient loadings have received limited attention, even given the fact that groundwater
605 in lake shore aquifers is usually concentrated in nutrients (Lewandowski et al.,
606 2015;Rosenberry et al., 2015). Even fewer studies focus on chemical budgets in the
607 proglacial lakes which are often difficult to access for sampling. Groundwater borne
608 DIN and DIP across the sediment-water interface in this study are determined with an
609 equation coupling the advective or LGD-derived, and diffusive solute transport
610 (Lerman et al., 1995;Hagerthey and Kerfoot, 1998)

$$611 \quad F_j = -nD_j^m \frac{dC_j}{dx} + v_{gw} C_j \quad (7)$$

612 where $-nD_j^m \frac{dC_j}{dx}$ is the diffusion input and $v_{gw} C_j$ is the LGD derived fluxes, F_j
613 [$\mu\text{M m}^{-2} \text{d}^{-1}$] is the mol flux of nutrient species j (representing DIN or DIP). n is the
614 sediment porosity. D_j^m is the molecular diffusion coefficient of nutrient species j ,

615 which is given to be $4.8 \times 10^{-5} \text{ m}^2 \text{ d}^{-1}$ for DIP (Quigley and Robbins, 1986), and $8.8 \times$
616 $10^{-5} \text{ m}^2 \text{ d}^{-1}$ for DIN (Li and Gregory, 1974), respectively. C_j [μM] is the
617 concentration of nutrient species j . x [m] is the sampling depth. v_{gw} is LGD rate
618 estimated by ^{222}Rn mass balance model and has a value of $10.3 \pm 8.2 \text{ mm d}^{-1}$. $\frac{dC_j}{dx}$ is
619 the concentration gradient of nutrient species j across the water-sedimentary interface.

620 Substituting the constants and the field data of DIN and DIP in to Equation 6, LGD
621 derived nutrient loadings are calculated to be $954.3 \mu\text{mol m}^{-2} \text{ d}^{-1}$ and $3.2 \mu\text{mol m}^{-2} \text{ d}^{-1}$
622 for DIN and DIP, respectively. Riverine inflow brings $1195.0 \mu\text{mol m}^{-2} \text{ d}^{-1}$ DIN, 52.9
623 $\mu\text{mol m}^{-2} \text{ d}^{-1}$ DIP into the lake. Lake water outflow derived nutrient loss is estimated
624 to be $1439.9 \mu\text{mol m}^{-2} \text{ d}^{-1}$ and $54.7 \mu\text{mol m}^{-2} \text{ d}^{-1}$ for DIN and DIP, respectively.
625 Nutrients in the lake can be also sourced from atmospheric deposit (mostly in form of
626 precipitation). With the nutrient concentrations in the rain water during the monitoring
627 period, the wet deposit is calculated to be $76 \mu\text{mol m}^{-2} \text{ d}^{-1}$ and $2.5 \mu\text{mol m}^{-2} \text{ d}^{-1}$, for
628 DIN and DIP, respectively. The loadings of DIN to the lakes are mainly from surface
629 runoff and LGD, which comprised of 42.9 % and 53.7 % of the total DIN loadings.
630 Groundwater derived DIP input, however, constitutes only 6.3 % of the total DIP
631 inputs to the lake, indicating groundwater borne DIP is less contributive to the
632 nutrient budget of the lake compared to DIN. Very recent studies on polar regions
633 have indicated that the glacier/snowpack water is the main N sources to the proglacial

634 lakes (Anderson et al., 2013;Dubnick et al., 2017). However, they do not consider the
635 contribution of groundwater borne N, in spite of the high groundwater connectivity in
636 the proglacial areas (Roy and Hayashi, 2008). This study stresses that groundwater
637 borne DIN could be comparable to the surface runoff derived DIN.

638 Based on nutrient results, the lake is considered to be an oligotrophic lake, similar
639 to other glacier melting dominant lakes in the QTP (Mitamura et al., 2003;Liu et al.,
640 2011).. Phytoplankton is good dissolved organic phosphate (DOP) recyclers and will
641 overcome inorganic P limitation though DOP cycling in most template lakes (Hudson
642 et al., 2000). However, this may be not applicable for the glacial melting water and
643 the peri/pro-glacial lake water. Previous studies show that phosphate nutrients are
644 dominated by DIP and particulate phosphate, and the DOP contributes less than 10 %
645 of the dissolved phosphate (Cole et al., 1998;Hawkings et al., 2016;Hodson, 2007).
646 Thus DOP recycling is not likely to low N: P ratio under these conditions. Thus, the
647 primary production (PP) is therefore considered to be controlled by the DIP loadings.
648 The sum of DIN and DIP inputs minus the calculated DIN and DIP outputs leads to
649 surpluses of $785.4 \mu\text{mol m}^{-2} \text{d}^{-1}$ and $3.9 \mu\text{mol m}^{-2} \text{d}^{-1}$ for DIN and DIP, respectively.
650 The surpluses are expected to be consumed by the phytoplankton and converted into
651 the PP under phosphate limited conditions. As primary producers in the fresh
652 lacustrine system consume the nutrient under variant N: P ratios (7.1 to 44.2, mean:

653 22.9) (Downing and McCauley, 1992), the biological uptake of DIN is roughly
654 estimated to be $89.3 \mu \text{M m}^2 \text{d}^{-1}$. Therefore, the nutrient budgets for DIN and DIP can
655 be finally conceptualized in Figures 8b and 8c.

656 4.6. Implications, prospective and limitations

657 Mountainous proglacial lakes are readily developed in glacier forefields of QTP and
658 other high mountainous glacial such as Europe Alps and Pamir at central Asian
659 (Heckmann et al. 2016). The proglacial lakes are always trapping system of sediment
660 and sinks for water and chemical originated from glacier/snowpack melting and
661 groundwater. In analogous to cosmogenic isotopes such as ^{10}Be serving as a tool to
662 quantify the sediment sources, approaches integrating ^{222}Rn and stable isotopes
663 provides both qualitatively and quantitatively evaluations of groundwater
664 contributions and hydrologic partitioning in these remote and untapped lacustrine
665 systems. Thus, it is expected that the multiple aqueous isotopes is considered to be
666 effective tools to investigate the LGD and hydrologic partitioning in other proglacial
667 lakes. This study is mainly limited by the relatively short sampling and monitoring
668 period. As a special hydrologic regime, the lake shore aquifers of the proglacial lakes
669 are experiencing frozen-unfrozen transition seasonally, and the dominant recharge of
670 glacial melting could be fluctuated significantly due to air temperature variation.
671 Therefore, future groundwater and hydrological studies can be extended to longtime

672 sampling and monitoring of stable isotopes and ^{222}Rn in different water endmembers
673 to reveal the seasonally hydrological and hydrogeological dynamics and their impacts
674 on local biogeochemical cycles and ecological systems. Special concerns would be
675 placed on how surface/groundwater interactions and the associated biogeochemical
676 processes in response to the seasonal frozen ground variations and glacier/snowpack
677 melting intensity.

678

679 **5. Conclusion**

680 A ^{222}Rn continuous monitoring is conducted at Ximen Co Lake, a proglacial lake
681 located at the east QTP. A dynamic ^{222}Rn mass balance model constrained by radium
682 mass balance and water level fluctuation is used to quantify temporal distribution of
683 LGD of the lake. The obtained LGD over the monitoring time ranges from -23.7
684 mm d^{-1} to 80.9 mm d^{-1} , with an average of $10.3 \pm 8.2 \text{ mm d}^{-1}$. Thereafter, a three
685 endmember model consisting of the budgets of water, stable isotopes and Cl^- is used
686 to depict the hydrologic partitioning of the lake. Riverine inflow, lake water outflow
687 via surface runoff, and surface evaporation are estimated to be 135.6 mm d^{-1} , 141.5
688 mm d^{-1} and 5.2 mm d^{-1} , respectively. LGD derived nutrient loading is estimated to be
689 $785.4 \mu\text{mol m}^{-2} \text{ d}^{-1}$ and $3.2 \mu\text{mol m}^{-2} \text{ d}^{-1}$ for DIN and DIP, respectively. This study also
690 implicates that LGD constitutes relatively small portion of the proglacial hydrologic

691 partitioning, however, delivers nearly a half of the nutrient loadings to the proglacial
692 lake.

693 This study presents the first attempt to quantify LGD and the associated nutrient
694 loadings to the proglacial lake of QTP. To our knowledge, there is almost no study on
695 the groundwater-lake water interaction in the high altitude proglacial lakes in QTP.

696 This study demonstrates that ^{222}Rn based approach can be used to investigate the
697 groundwater dynamics in the high altitude proglacial lakes. The method is
698 instructional to similar studies in other proglacial lakes in the QTP and elsewhere. For
699 a comprehensive understanding the hydrological and biogeochemical dynamics in the
700 QTP, interdisciplinary and multi-approach integrated studies are in great need. Of
701 particular importance are the lake hydrology and groundwater surface water
702 interaction studies based on multiple approaches such as remote sensing products,
703 long term and high resolution observation of climatological parameters and isotopic
704 data.

705

706 **Acknowledgements**

707 This study was supported by grants from the National Natural Science Foundation of
708 China (NSFC, No.41572208) and (NSFC, 91747204), and the Research Grants
709 Council of Hong Kong Special Administrative Region, China (HKU17304815), and

710 the seed fund programed granted by HKU-ZIRI. The authors thank Mr. Buming Jiang
711 for his kind help in the field works during the campaign and Ergang Lian for his help
712 in stable isotope analysis. The authors thank Jessie Lai for her help in FIA analysis in
713 School of Biological Sciences, HKU. Supporting data are included as in the files of
714 supplementary information 2 and 3; Climatological data are purchased through
715 <http://www.weatherdt.com/shop.html>; any additional data may be obtained from L.X.
716 (email: xinluo@hku.hk);

717 **References**

- 718 Åberg, J., Jansson, M., and Jonsson, A.: Importance of water temperature and
719 thermal stratification dynamics for temporal variation of surface water CO₂ in a
720 boreal lake, *Journal of Geophysical Research: Biogeosciences* (2005–2012), 115,
721 10.1029/2009JG001085, 2010.
- 722 Andermann, C., Longuevergne, L., Bonnet, S., Crave, A., Davy, P., and Gloaguen, R.:
723 Impact of transient groundwater storage on the discharge of Himalayan rivers, *Nat*
724 *Geosci*, 5, 127-132, Doi 10.1038/Ngeo1356, 2012.
- 725 Anderson, L., Birks, J., Rover, J., and Guldager, N.: Controls on recent Alaskan lake
726 changes identified from water isotopes and remote sensing, *Geophysical Research*
727 *Letters*, 40, 3413-3418, 2013.
- 728 Anderson, N. J., Saros, J. E., Bullard, J. E., Cahoon, S. M., McGowan, S., Bagshaw, E. A.,
729 Barry, C. D., Bindler, R., Burpee, B. T., and Carrivick, J. L.: The Arctic in the Twenty-First
730 Century: Changing Biogeochemical Linkages across a Paraglacial Landscape of
731 Greenland, *BioScience*, 67, 118-133, 2017.
- 732 Barry, R. G.: The status of research on glaciers and global glacier recession: a review,
733 *Progress in Physical Geography*, 30, 285-306, 2006.
- 734 Batlle-Aguilar, J., Harrington, G. A., Leblanc, M., Welch, C., and Cook, P. G.: Chemistry
735 of groundwater discharge inferred from longitudinal river sampling, *Water Resour*
736 *Res*, 50, 1550-1568, 10.1002/2013WR013591, 2014.
- 737 Belanger, T. V., Mikutel, D. F., and Churchill, P. A.: Groundwater seepage nutrient
738 loading in a Florida Lake, *Water Res*, 19, 773-781,
739 [http://dx.doi.org/10.1016/0043-1354\(85\)90126-5](http://dx.doi.org/10.1016/0043-1354(85)90126-5), 1985.

740 Biskop, S., Maussion, F., Krause, P., and Fink, M.: Differences in the water-balance
741 components of four lakes in the southern-central Tibetan Plateau, *Hydrol Earth Syst*
742 *Sc*, 20, 209, 2016.

743 Blume, T., Krause, S., Meinikmann, K., and Lewandowski, J.: Upscaling lacustrine
744 groundwater discharge rates by fiber-optic distributed temperature sensing, *Water*
745 *Resour Res*, 49, 7929-7944, 10.1002/2012WR013215, 2013.

746 Böhner, J.: Säkulare Klimaschwankungen und rezente Klimatrends Zentral-und
747 Hochasiens, Goltze, 1996.

748 Böhner, J.: General climatic controls and topoclimatic variations in Central and High
749 Asia, *Boreas*, 35, 279-295, 2006.

750 Bolch, T., Kulkarni, A., Kääh, A., Huggel, C., Paul, F., Cogley, J. G., Frey, H., Kargel, J. S.,
751 Fujita, K., Scheel, M., Bajracharya, S., and Stoffel, M.: The State and Fate of
752 Himalayan Glaciers, *Science*, 336, 310-314, 2012.

753 Brown, L. E., Hannah, D. M., Milner, A. M., Soulsby, C., Hodson, A. J., and Brewer, M.
754 J.: Water source dynamics in a glacierized alpine river basin (Taillon-Gabiétous,
755 French Pyrénées), *Water Resour Res*, 42, 2006.

756 Burnett, W. C., Peterson, R. N., Santos, I. R., and Hicks, R. W.: Use of automated radon
757 measurements for rapid assessment of groundwater flow into Florida streams,
758 *Journal of Hydrology*, 380, 298-304, 2010.

759 Callegary, J. B., Kikuchi, C. P., Koch, J. C., Lilly, M. R., and Leake, S. A.: Review:
760 Groundwater in Alaska (USA), *Hydrogeol J*, 21, 25-39, 10.1007/s10040-012-0940-5,
761 2013.

762 Cole, J., Nina, J., and Caraco, F.: Atmospheric exchange of carbon dioxide in a
763 low-wind oligotrophic lake measured by the addition of SF₆, *Limnol Oceanogr*, 43,
764 647-656, 1998.

765 Cook, P., Lamontagne, S., Berhane, D., and Clark, J.: Quantifying groundwater
766 discharge to Cockburn River, southeastern Australia, using dissolved gas tracers
767 222Rn and SF₆, *Water Resour Res*, 42, 2006.

768 Cook, P. G., Favreau, G., Dighton, J. C., and Tickell, S.: Determining natural
769 groundwater influx to a tropical river using radon, chlorofluorocarbons and ionic
770 environmental tracers, *Journal of Hydrology*, 277, 74-88,
771 [http://dx.doi.org/10.1016/S0022-1694\(03\)00087-8](http://dx.doi.org/10.1016/S0022-1694(03)00087-8), 2003.

772 Corbett, D. R., Burnett, W. C., Cable, P. H., and Clark, S. B.: Radon tracing of
773 groundwater input into Par Pond, Savannah River site, *Journal of Hydrology*, 203,
774 209-227, 1997.

775 Cui, X., Ren, J., Qin, X., Sun, W., Yu, G., Wang, Z., and Liu, W.: Chemical characteristics
776 and environmental records of a snow-pit at the Glacier No. 12 in the Laohugou Valley,
777 Qilian Mountains, *Journal of Earth Science*, 25, 379-385, 2014.

778 Dansgaard, W.: Stable isotopes in precipitation, *Tellus A*, 16, 1964.

779 Dimova, N., Paytan, A., Kessler, J. D., Sparrow, K., Garcia-Tigreros Kodovska, F., Lecher,
780 A. L., Murray, J., and Tulaczyk, S. M.: The current magnitude and mechanisms of
781 groundwater discharge in the Arctic: a case study from Alaska, *Environ Sci Technol*,
782 49, 12036-12043, 2015.

783 Dimova, N. T., and Burnett, W. C.: Evaluation of groundwater discharge into small
784 lakes based on the temporal distribution of radon-222, *Limnol. Oceanogr*, 56,
785 486-494, 2011.

786 Dimova, N. T., Burnett, W. C., Chanton, J. P., and Corbett, J. E.: Application of
787 radon-222 to investigate groundwater discharge into small shallow lakes, *Journal of*
788 *Hydrology*, 2013.

789 Downing, J. A., and McCauley, E.: The nitrogen: phosphorus relationship in lakes,
790 *Limnol Oceanogr*, 37, 936-945, 1992.

791 Dubnick, A., Wadham, J., Tranter, M., Sharp, M., Orwin, J., Barker, J., Bagshaw, E., and
792 Fitzsimons, S.: Trickle or treat: The dynamics of nutrient export from polar glaciers,
793 *Hydrol Process*, 31, 1776-1789, 10.1002/hyp.11149, 2017.

794 Einarsdottir, K., Wallin, M. B., and Sobek, S.: High terrestrial carbon load via
795 groundwater to a boreal lake dominated by surface water inflow, *Journal of*
796 *Geophysical Research: Biogeosciences*, 122 (1), 15-29, 10.1002/2016JG003495, 2017.

797 Farinotti, D., Longuevergne, L., Moholdt, G., Duethmann, D., Molg, T., Bolch, T.,
798 Vorogushyn, S., and Guntner, A.: Substantial glacier mass loss in the Tien Shan over
799 the past 50 years, *Nature Geosci*, 8, 716-722, 10.1038/ngeo2513
800 [http://www.nature.com/ngeo/journal/v8/n9/abs/ngeo2513.html#supplementary-inf](http://www.nature.com/ngeo/journal/v8/n9/abs/ngeo2513.html#supplementary-information)
801 [ormation](http://www.nature.com/ngeo/journal/v8/n9/abs/ngeo2513.html#supplementary-inf), 2015.

802 Gat, J.: Stable isotopes of fresh and saline lakes, in: *Physics and chemistry of lakes*,
803 Springer, 139-165, 1995.

804 Gat, J.: Oxygen and hydrogen isotopes in the hydrologic cycle, *Annual Review of Earth*
805 *and Planetary Sciences*, 24, 225-262, 1996.

806 Genereux, D.: Quantifying uncertainty in tracer-based hydrograph separations, *Water*
807 *Resour Res*, 34, 915-919, 1998.

808 Gibson, J., Edwards, T., Burse, G., and Prowse, T.: Estimating evaporation using stable
809 isotopes: quantitative results and sensitivity analysis for, *Nordic Hydrology*, 24, 79-94,
810 1993.

811 Gibson, J. J.: Short-term evaporation and water budget comparisons in shallow Arctic
812 lakes using non-steady isotope mass balance, *Journal of Hydrology*, 264, 242-261,
813 2002.

814 Gibson, J. J., and Edwards, T. W. D.: Regional water balance trends and
815 evaporation-transpiration partitioning from a stable isotope survey of lakes in

816 northern Canada, *Global Biogeochem Cy*, 16, 10-11-10-14, 10.1029/2001GB001839,
817 2002.

818 Gibson, J. J., Birks, S. J., and Yi, Y.: Stable isotope mass balance of lakes: a
819 contemporary perspective, *Quaternary Science Reviews*, 131, Part B, 316-328,
820 <http://dx.doi.org/10.1016/j.quascirev.2015.04.013>, 2016.

821 Gilfedder, B., Frei, S., Hofmann, H., and Cartwright, I.: Groundwater discharge to
822 wetlands driven by storm and flood events: Quantification using continuous
823 Radon-222 and electrical conductivity measurements and dynamic mass-balance
824 modelling, *Geochim Cosmochim Ac*, 165, 161-177, 2015.

825 Gonfiantini, R.: Environmental isotopes in lake studies, *Handbook of environmental*
826 *isotope geochemistry*, 2, 113-168, 1986.

827 Good, S. P., Noone, D., and Bowen, G.: Hydrologic connectivity constrains partitioning
828 of global terrestrial water fluxes, *Science*, 349, 175-177, 10.1126/science.aaa5931,
829 2015.

830 Hagerthey, S. E., and Kerfoot, W. C.: Groundwater flow influences the biomass and
831 nutrient ratios of epibenthic algae in a north temperate seepage lake, *Limnol*
832 *Oceanogr*, 43, 1227-1242, 1998.

833 Harris, C., Arenson, L. U., Christiansen, H. H., Etzelmüller, B., Frauenfelder, R., Gruber,
834 S., Haeberli, W., Hauck, C., Hölzle, M., and Humlum, O.: Permafrost and climate in
835 Europe: Monitoring and modelling thermal, geomorphological and geotechnical
836 responses, *Earth-Science Reviews*, 92, 117-171, 2009.

837 Hasler, C. T., Midway, S. R., Jeffrey, J. D., Tix, J. A., Sullivan, C., and Suski, C. D.:
838 Exposure to elevated pCO₂ alters post-treatment diel movement patterns of
839 largemouth bass over short time scales, *Freshwater Biology*, 61, 1590-1600,
840 10.1111/fwb.12805, 2016.

841 Hawkings, J., Wadham, J., Tranter, M., Telling, J., Bagshaw, E., Beaton, A., Simmons, S.
842 L., Chandler, D., Tedstone, A., and Nienow, P.: The Greenland Ice Sheet as a hot spot
843 of phosphorus weathering and export in the Arctic, *Global Biogeochem Cy*, 30 (2),
844 191-210, 2016.

845 Heckmann, T., McColl, S., and Morche, D.: Retreating ice: research in pro-glacial areas
846 matters, *Earth Surface Processes and Landforms*, 41, 271-276, 10.1002/esp.3858,
847 2016.

848 Hodson, A., Mumford, P., Kohler, J., and Wynn, P. M.: The High Arctic glacial
849 ecosystem: new insights from nutrient budgets, *Biogeochemistry*, 72, 233-256, 2005.

850 Hodson, A.: Phosphorus in glacial meltwaters, *Glacier Science and Environmental*
851 *Change*, 81-82, 2007.

852 Hood, J. L., Roy, J. W., and Hayashi, M.: Importance of groundwater in the water
853 balance of an alpine headwater lake, *Geophysical Research Letters*, 33,

854 10.1029/2006GL026611, 2006.

855 Hren, M. T., Bookhagen, B., Blisniuk, P. M., Booth, A. L., and Chamberlain, C. P.: $\delta^{18}\text{O}$
856 and δD of streamwaters across the Himalaya and Tibetan Plateau: Implications for
857 moisture sources and paleoelevation reconstructions, *Earth Planet Sc Lett*, 288,
858 20-32, 2009.

859 Hudson, J. J., Taylor, W. D., and Schindler, D. W.: Phosphate concentrations in lakes,
860 *Nature*, 406, 54-56, 2000.

861 Johannes, R. E.: The Ecological Significance of the Submarine Discharge of
862 Groundwater, *Mar Ecol-Prog Ser*, 3, 365-373, 1980.

863 Kim, G., Burnett, W. C., Dulaiova, H., Swarzenski, P. W., and Moore, W. S.:
864 Measurement of Ra-224 and Ra-226 activities in natural waters using a radon-in-air
865 monitor, *Environ Sci Technol*, 35, 4680-4683, 2001.

866 Klaus, J., and McDonnell, J.: Hydrograph separation using stable isotopes: Review and
867 evaluation, *Journal of Hydrology*, 505, 47-64, 2013.

868 Kluge, T., Ilmberger, J., Rohden, C. v., and Aeschbach-Hertig, W.: Tracing and
869 quantifying groundwater inflow into lakes using a simple method for radon-222
870 analysis, *Hydrol Earth Syst Sc*, 11, 1621-1631, 2007.

871 Kluge, T., von Rohden, C., Sonntag, P., Lorenz, S., Wieser, M., Aeschbach-Hertig, W.,
872 and Ilmberger, J.: Localising and quantifying groundwater inflow into lakes using
873 high-precision ^{222}Rn profiles, *Journal of Hydrology*, 450, 70-81, 2012.

874 Kraemer, T. F.: Radium isotopes in Cayuga Lake, New York: Indicators of inflow and
875 mixing processes, *Limnol Oceanogr*, 50, 158-168, 2005.

876 LaBaugh, J. W., Rosenberry, D. O., and Winter, T. C.: Groundwater contribution to the
877 water and chemical budgets of Williams Lake, Minnesota, 1980-1991, *Can J Fish*
878 *Aquat Sci*, 52, 754-767, 1995.

879 LaBaugh, J. W., Winter, T. C., Rosenberry, D. O., Schuster, P. F., Reddy, M. M., and
880 Aiken, G. R.: Hydrological and chemical estimates of the water balance of a closed-
881 basin lake in north central Minnesota, *Water Resour Res*, 33, 2799-2812, 1997.

882 Langston, G., Hayashi, M., and Roy, J. W.: Quantifying groundwater-surface water
883 interactions in a proglacial moraine using heat and solute tracers, *Water Resour Res*,
884 49, 5411-5426, 10.1002/wrcr.20372, 2013.

885 Lazar, B., Weinstein, Y., Paytan, A., Magal, E., Bruce, D., and Kolodny, Y.: Ra and Th
886 adsorption coefficients in lakes—Lake Kinneret (Sea of Galilee)“natural experiment”,
887 *Geochim Cosmochim Ac*, 72, 3446-3459, 2008.

888 Lazhu, Yang, K., Wang, J., Lei, Y., Chen, Y., Zhu, L., Ding, B., and Qin, J.: Quantifying
889 evaporation and its decadal change for Lake Nam Co, central Tibetan Plateau, *Journal*
890 *of Geophysical Research (Atmospheres)*, 121, 7578-7591, 2016.

891 Lecher, A. L., Kessler, J., Sparrow, K., Garcia-Tigreros Kodovska, F., Dimova, N., Murray,

892 J., Tulaczyk, S., and Paytan, A.: Methane transport through submarine groundwater
893 discharge to the North Pacific and Arctic Ocean at two Alaskan sites, *Limnol Oceanogr*,
894 61 (S1), S344-355, 2015.

895 Lee, C. M., Jiao, J. J., Luo, X., and Moore, W. S.: Estimation of submarine groundwater
896 discharge and associated nutrient fluxes in Tolo Harbour, Hong Kong, *Sci Total Environ*,
897 433, 427-433, 10.1016/j.scitotenv.2012.06.073, 2012.

898 Lee, D. R.: A device for measuring seepage flux in lakes and estuaries, *Limnol*
899 *Oceanogr*, 22, 140-147, 1977.

900 Lee, D. R., Cherry, J. A., and Pickens, J. F.: Groundwater transport of a salt tracer
901 through a sandy lakebed, *Limnol Oceanogr*, 25, 45-61, 1980.

902 Lehmkuhl, F.: Extent and spatial distribution of Pleistocene glaciations in eastern
903 Tibet, *Quatern Int*, 45-46, 123-134,
904 [http://dx.doi.org/10.1016/S1040-6182\(97\)00010-4](http://dx.doi.org/10.1016/S1040-6182(97)00010-4), 1998.

905 Lei, Y., Yao, T., Yang, K., Sheng, Y., Kleinherenbrink, M., Yi, S., Bird, B. W., Zhang, X.,
906 Zhu, L., and Zhang, G.: Lake seasonality across the Tibetan Plateau and their varying
907 relationship with regional mass changes and local hydrology, *Geophysical Research*
908 *Letters*, 44, 892-900, 2017.

909 Lemieux, J. M., Sudicky, E. A., Peltier, W. R., and Tarasov, L.: Dynamics of groundwater
910 recharge and seepage over the Canadian landscape during the Wisconsinian
911 glaciation, *Journal of Geophysical Research: Earth Surface (2003–2012)*, 113,
912 10.1029/2007JF000838, 2008a.

913 Lemieux, J. M., Sudicky, E. A., Peltier, W. R., and Tarasov, L.: Simulating the impact of
914 glaciations on continental groundwater flow systems: 1. Relevant processes and
915 model formulation, *Journal of Geophysical Research: Earth Surface*, 113, n/a-n/a,
916 10.1029/2007JF000928, 2008b.

917 Lemieux, J. M., Sudicky, E. A., Peltier, W. R., and Tarasov, L.: Simulating the impact of
918 glaciations on continental groundwater flow systems: 2. Model application to the
919 Wisconsinian glaciation over the Canadian landscape, *Journal of Geophysical*
920 *Research: Earth Surface (2003–2012)*, 113, 10.1029/2007JF000929, 2008c.

921 Lerman, A., Imboden, D., and Gat, J.: *Physics and chemistry of lakes*, New York, 1995.

922 Levy, A., Robinson, Z., Krause, S., Waller, R., and Weatherill, J.: Long-term variability
923 of proglacial groundwater-fed hydrological systems in an area of glacier retreat,
924 Skeiðarársandur, Iceland, *Earth Surface Processes and Landforms*, 40, 981-994,
925 10.1002/esp.3696, 2015.

926 Lewandowski, J., Meinikmann, K., Ruhtz, T., Pöschke, F., and Kirillin, G.: Localization of
927 lacustrine groundwater discharge (LGD) by airborne measurement of thermal
928 infrared radiation, *Remote Sens Environ*, 138, 119-125,
929 <http://dx.doi.org/10.1016/j.rse.2013.07.005>, 2013.

930 Lewandowski, J., Meinikmann, K., Nützmann, G., and Rosenberry, D. O.: Groundwater
931 – the disregarded component in lake water and nutrient budgets. Part 2: effects of
932 groundwater on nutrients, *Hydrol Process*, 29, 2922-2955, 10.1002/hyp.10384, 2015.

933 Li, Y. H., and Gregory, S.: Diffusion of Ions in Sea-Water and in Deep-Sea Sediments,
934 *Geochim Cosmochim Ac*, 38, 703-714, 1974.

935 Liu, C., Liu, J., Wang, X. S., and Zheng, C.: Analysis of groundwater–lake interaction by
936 distributed temperature sensing in Badain Jaran Desert, Northwest China, *Hydrol*
937 *Process*, 30 (9), 1330-1341, 2015.

938 Liu, Y., Yao, T., Jiao, N., Tian, L., Hu, A., Yu, W., and Li, S.: Microbial diversity in the
939 snow, a moraine lake and a stream in Himalayan glacier, *Extremophiles*, 15, 411-421,
940 2011.

941 Luo, X., Jiao, J. J., Moore, W., and Lee, C. M.: Submarine groundwater discharge
942 estimation in an urbanized embayment in Hong Kong via short-lived radium isotopes
943 and its implication of nutrient loadings and primary production, *Mar Pollut Bull*, 82,
944 144-154, 2014.

945 Luo, X., and Jiao, J. J.: Submarine groundwater discharge and nutrient loadings in Tolo
946 Harbor, Hong Kong using multiple geotracer-based models, and their implications of
947 red tide outbreaks, *Water Res*, 102, 11-31,
948 <http://dx.doi.org/10.1016/j.watres.2016.06.017>, 2016.

949 Luo, X., Jiao, J. J., Wang, X.-s., and Liu, K.: Temporal ²²²Rn distributions to reveal
950 groundwater discharge into desert lakes: implication of water balance in the Badain
951 Jaran Desert, China, *Journal of Hydrology*, 534, 87-103, 2016.

952 Luo, X., Jiao, J. J., Wang, X.-s., Liu, K., Lian, E., and Yang, S.: Groundwater discharge
953 and hydrologic partition of the lakes in desert environment: Insights from stable
954 ¹⁸O/²H and radium isotopes, *Journal of Hydrology*, 546, 189-203, 2017.

955 Luo, X., Jiao, J. J., Liu, Y., Zhang, X., Liang, W., and Tang, D.: Evaluation of Water
956 Residence Time, Submarine Groundwater Discharge, and Maximum New Production
957 Supported by Groundwater Borne Nutrients in a Coastal Upwelling Shelf System,
958 *Journal of Geophysical Research: Oceans*, 123, 631-655, 2018.

959 Ma, N., Zhang, Y., Szilagyi, J., Guo, Y., Zhai, J., and Gao, H.: Evaluating the
960 complementary relationship of evapotranspiration in the alpine steppe of the
961 Tibetan Plateau, *Water Resour Res*, 51, 1069-1083, 10.1002/2014WR015493, 2015.

962 MacIntyre, S., Wannikhof, R., Chanton, J. P., Matson, P. A., and Hariss, R. C.: Biogenic
963 Trace Gases: Measuring Emissions from Soil and Water, 52 pp., 1995.

964 Magnusson, J., Kobierska, F., Huxol, S., Hayashi, M., Jonas, T., and Kirchner, J. W.: Melt
965 water driven stream and groundwater stage fluctuations on a glacier forefield
966 (Dammagletscher, Switzerland), *Hydrol Process*, 28, 823-836, 2014.

967 Mitamura, O., Seike, Y., Kondo, K., Goto, N., Anbutsu, K., Akatsuka, T., Kihira, M.,

968 Tsering, T. Q., and Nishimura, M.: First investigation of ultraoligotrophic alpine Lake
969 Puma Yumco in the pre-Himalayas, China, *Limnology*, 4, 167-175, 2003.

970 Moore, W. S.: Sampling radium-228 in the deep ocean, *Deep Sea Res.*, 23, 647-651,
971 1976.

972 Nakayama, T., and Watanabe, M.: Missing role of groundwater in water and nutrient
973 cycles in the shallow eutrophic Lake Kasumigaura, Japan, *Hydrol Process*, 22,
974 1150-1172, 2008.

975 Paytan, A., Lecher, A. L., Dimova, N., Sparrow, K. J., Kodovska, F. G.-T., Murray, J.,
976 Tulaczyk, S., and Kessler, J. D.: Methane transport from the active layer to lakes in the
977 Arctic using Toolik Lake, Alaska, as a case study, *Proceedings of the National Academy
978 of Sciences*, 112, 3636-3640, 2015.

979 Qiu, J.: China: the third pole, *Nature News*, 454, 393-396, 2008.

980 Quigley, M. A., and Robbins, J. A.: Phosphorus release processes in nearshore
981 southern Lake Michigan, *Can J Fish Aquat Sci*, 43, 1201-1207, 1986.

982 Ren, W., Yao, T., Yang, X., and Joswiak, D. R.: Implications of variations in $\delta^{18}\text{O}$ and δD
983 in precipitation at Madoi in the eastern Tibetan Plateau, *Quatern Int*, 313-314, 56-61,
984 <https://doi.org/10.1016/j.quaint.2013.05.026>, 2013.

985 Ren, W., Yao, T., Xie, S., and He, Y.: Controls on the stable isotopes in precipitation
986 and surface waters across the southeastern Tibetan Plateau, *Journal of Hydrology*,
987 545, 276-287, <http://dx.doi.org/10.1016/j.jhydrol.2016.12.034>, 2017.

988 Rosenberry, D. O., Lewandowski, J., Meinikmann, K., and Nützmann, G.:
989 Groundwater-the disregarded component in lake water and nutrient budgets. Part 1:
990 effects of groundwater on hydrology, *Hydrol Process*, 29, 2895-2921, 2015.

991 Roy, J. W., and Hayashi, M.: Groundwater exchange with two small alpine lakes in the
992 Canadian Rockies, *Hydrol Process*, 22, 2838-2846, 2008.

993 Schafran, G. C., and Driscoll, C. T.: Flow path - composition relationships for
994 groundwater entering an acidic lake, *Water Resour Res*, 29, 145-154, 1993.

995 Scheidegger, J. M., and Bense, V. F.: Impacts of glacially recharged groundwater flow
996 systems on talik evolution, *Journal of Geophysical Research: Earth Surface*, 119,
997 758-778, 10.1002/2013JF002894, 2014.

998 Schlutz, F., and Lehmkuhl, F.: Holocene climatic change and the nomadic
999 Anthropocene in Eastern Tibet: palynological and geomorphological results from the
1000 Nianbaoyeze Mountains, *Quaternary Science Reviews*, 28, 1449-1471, 2009.

1001 Schmidt, A., Gibson, J. J., Santos, I. R., Schubert, M., Tattrie, K., and Weiss, H.: The
1002 contribution of groundwater discharge to the overall water budget of two typical
1003 Boreal lakes in Alberta/Canada estimated from a radon mass balance, *Hydrol Earth
1004 Syst Sc*, 14, 79-89, 2010.

1005 Sebok, E., Duque, C., Kazmierczak, J., Engesgaard, P., Nilsson, B., Karan, S., and

1006 Frandsen, M.: High-resolution distributed temperature sensing to detect seasonal
1007 groundwater discharge into Lake Væng, Denmark, *Water Resour Res*, 49, 5355-5368,
1008 2013.

1009 Shaw, R. D., and Prepas, E. E.: Groundwater-lake interactions: I. Accuracy of seepage
1010 meter estimates of lake seepage, *Journal of Hydrology*, 119, 105-120,
1011 [http://dx.doi.org/10.1016/0022-1694\(90\)90037-X](http://dx.doi.org/10.1016/0022-1694(90)90037-X), 1990.

1012 Slaymaker, O.: Criteria to distinguish between periglacial, proglacial and paraglacial
1013 environments, *Quaestiones Geographicae*, 30, 85-94, 2011.

1014 Slomp, C. P., and Van Cappellen, P.: Nutrient inputs to the coastal ocean through
1015 submarine groundwater discharge: controls and potential impact, *Journal of*
1016 *Hydrology*, 295, 64-86, Doi 10.1016/J.Jhyfrol.2004.02.018, 2004.

1017 Smerdon, B., Mendoza, C., and Devito, K.: Simulations of fully coupled lake-
1018 groundwater exchange in a subhumid climate with an integrated hydrologic model,
1019 *Water Resour Res*, 43, 2007.

1020 Stets, E. G., Winter, T. C., Rosenberry, D. O., and Striegl, R. G.: Quantification of
1021 surface water and groundwater flows to open- and closed-basin lakes in a
1022 headwaters watershed using a descriptive oxygen stable isotope model, *Water*
1023 *Resour Res*, 46, 10.1029/2009WR007793, 2010.

1024 Tockner, K., Malard, F., Uehlinger, U., and Ward, J.: Nutrients and organic matter in a
1025 glacial river-floodplain system (Val Roseg, Switzerland), *Limnol Oceanogr*, 47, 266-277,
1026 2002.

1027 Valiela, I., Teal, J. M., Volkmann, S., Shafer, D., and Carpenter, E. J.: Nutrient and
1028 Particulate Fluxes in a Salt-Marsh Ecosystem - Tidal Exchanges and Inputs by
1029 Precipitation and Groundwater, *Limnol Oceanogr*, 23, 798-812, 1978.

1030 Wang, C., Dong, Z., Qin, X., Zhang, J., Du, W., and Wu, J.: Glacier meltwater runoff
1031 process analysis using δD and $\delta^{18}O$ isotope and chemistry at the remote Laohugou
1032 glacier basin in western Qilian Mountains, China, *Journal of Geographical Sciences*,
1033 26, 722-734, 2016a.

1034 Wang, J., Zhu, L., Wang, Y., Ju, J., Xie, M., and Daut, G.: Comparisons between the
1035 chemical compositions of lake water, inflowing river water, and lake sediment in Nam
1036 Co, central Tibetan Plateau, China and their controlling mechanisms, *Journal of Great*
1037 *Lakes Research*, 36, 587-595, 2010.

1038 Wang, R., Liu, Z., Jiang, L., Yao, Z., Wang, J., and Ju, J.: Comparison of surface water
1039 chemistry and weathering effects of two lake basins in the Changtang Nature Reserve,
1040 China, *Journal of Environmental Sciences*, 41, 183-194,
1041 <http://dx.doi.org/10.1016/j.jes.2015.03.016>, 2016b.

1042 Wang, S.: Frozen ground and environment in the Zoige Plateau and its surrounding
1043 mountains (In Chinese with English abstract), *Journal of Glaciology and Geocryology*,

1044 19, 39-46, 1997.

1045 Warner, N. R., Christie, C. A., Jackson, R. B., and Vengosh, A.: Impacts of shale gas
1046 wastewater disposal on water quality in western Pennsylvania, *Environ Sci Technol*,
1047 47, 11849-11857, 2013.

1048 Weynell, M., Wiechert, U., and Zhang, C.: Chemical and isotopic (O, H, C) composition
1049 of surface waters in the catchment of Lake Donggi Cona (NW China) and implications
1050 for paleoenvironmental reconstructions, *Chemical Geology*, 435, 92-107,
1051 <http://dx.doi.org/10.1016/j.chemgeo.2016.04.012>, 2016.

1052 White, D., Lapworth, D. J., Stuart, M. E., and Williams, P. J.: Hydrochemical profiles in
1053 urban groundwater systems: New insights into contaminant sources and pathways in
1054 the subsurface from legacy and emerging contaminants, *Sci Total Environ*, 562,
1055 962-973, <http://dx.doi.org/10.1016/j.scitotenv.2016.04.054>, 2016.

1056 Wilson, J., and Rocha, C.: A combined remote sensing and multi-tracer approach for
1057 localising and assessing groundwater-lake interactions, *International Journal of*
1058 *Applied Earth Observation and Geoinformation*, 44, 195-204, 2016.

1059 Winter, T. C.: Relation of streams, lakes, and wetlands to groundwater flow systems,
1060 *Hydrogeol J*, 7, 28-45, 1999.

1061 Wischniewski, J., Herzschuh, U., Rühland, K. M., Bräuning, A., Mischke, S., Smol, J. P.,
1062 and Wang, L.: Recent ecological responses to climate variability and human impacts
1063 in the Nianbaoyeze Mountains (eastern Tibetan Plateau) inferred from pollen, diatom
1064 and tree-ring data, *Journal of paleolimnology*, 51, 287-302, 2014.

1065 Xin, W., Yongjian, D., Shiyin, L., Lianghong, J., Kunpeng, W., Zongli, J., and Wanqin, G.:
1066 Changes of glacial lakes and implications in Tian Shan, central Asia, based on remote
1067 sensing data from 1990 to 2010, *Environmental Research Letters*, 8, 044052, 2013.

1068 Yang, K., Wu, H., Qin, J., Lin, C., Tang, W., and Chen, Y.: Recent climate changes over
1069 the Tibetan Plateau and their impacts on energy and water cycle: A review, *Global*
1070 *and Planetary Change*, 112, 79-91, 2014.

1071 Yao, T., Thompson, L., Yang, W., Yu, W., Gao, Y., Guo, X., Yang, X., Duan, K., Zhao, H.,
1072 Xu, B., Pu, J., Lu, A., Xiang, Y., Kattel, D. B., and Joswiak, D.: Different glacier status
1073 with atmospheric circulations in Tibetan Plateau and surroundings, *Nature Clim.*
1074 *Change*, 2, 663-667,
1075 [http://www.nature.com/nclimate/journal/v2/n9/abs/nclimate1580.html#supplemen](http://www.nature.com/nclimate/journal/v2/n9/abs/nclimate1580.html#supplementary-information)
1076 *tary-information*, 2012.

1077 Yao, T., Masson-Delmotte, V., Gao, J., Yu, W., Yang, X., Risi, C., Sturm, C., Werner, M.,
1078 Zhao, H., He, Y., Ren, W., Tian, L., Shi, C., and Hou, S.: A review of climatic controls on
1079 $\delta^{18}\text{O}$ in precipitation over the Tibetan Plateau: Observations and simulations,
1080 *Reviews of Geophysics*, 51, 525-548, 10.1002/rog.20023, 2013.

1081 Yao, Z., Wang, R., Liu, Z., Wu, S., and Jiang, L.: Spatial-temporal patterns of major ion

1082 chemistry and its controlling factors in the Manasarovar Basin, Tibet, *Journal of*
1083 *Geographical Sciences*, 25, 687-700, 10.1007/s11442-015-1196-5, 2015.

1084 Yuan, H., Liu, E., Shen, J., Zhou, H., Geng, Q., and An, S.: Characteristics and origins of
1085 heavy metals in sediments from Ximen Co Lake during summer monsoon season, a
1086 deep lake on the eastern Tibetan Plateau, *J Geochem Explor*, 136, 76-83,
1087 <http://dx.doi.org/10.1016/j.gexplo.2013.10.008>, 2014.

1088 Zhang, B., Wu, Y., Zhu, L., Wang, J., Li, J., and Chen, D.: Estimation and trend
1089 detection of water storage at Nam Co Lake, central Tibetan Plateau, *Journal of*
1090 *Hydrology*, 405, 161-170, 2011.

1091 Zhang, C., and Mischke, S.: A Lateglacial and Holocene lake record from the
1092 Nianbaoyeze Mountains and inferences of lake, glacier and climate evolution on the
1093 eastern Tibetan Plateau, *Quaternary Science Reviews*, 28, 1970-1983, 2009.

1094 Zhang, G., Yao, T., Xie, H., Kang, S., and Lei, Y.: Increased mass over the Tibetan
1095 Plateau: from lakes or glaciers?, *Geophysical Research Letters*, 40, 2125-2130, 2013.

1096 Zhang, G., Yao, T., Piao, S., Bolch, T., Xie, H., Chen, D., Gao, Y., O'Reilly, C. M., Shum, C.,
1097 and Yang, K.: Extensive and drastically different alpine lake changes on Asia's high
1098 plateaus during the past four decades, *Geophysical Research Letters*, 44, 252-260,
1099 2017a.

1100 Zhang, G., Yao, T., Shum, C., Yi, S., Yang, K., Xie, H., Feng, W., Bolch, T., Wang, L., and
1101 Behrangi, A.: Lake volume and groundwater storage variations in Tibetan Plateau's
1102 endorheic basin, *Geophysical Research Letters*, 44, 5550-5560, 2017b.

1103 Zhang, Y., Liu, C., Tang, Y., and Yang, Y.: Trends in pan evaporation and reference and
1104 actual evapotranspiration across the Tibetan Plateau, *Journal of Geophysical*
1105 *Research: Atmospheres* (1984–2012), 112, 10.1029/2006JD008161, 2007.

1106 Zhou, S., Kang, S., Chen, F., and Joswiak, D. R.: Water balance observations reveal
1107 significant subsurface water seepage from Lake Nam Co, south-central Tibetan
1108 Plateau, *Journal of Hydrology*, 491, 89-99, 2013.

1109 Zlotnik, V. A., Olaguera, F., and Ong, J. B.: An approach to assessment of flow regimes
1110 of groundwater-dominated lakes in arid environments, *Journal of hydrology*, 371,
1111 22-30, 2009.

1112 Zlotnik, V. A., Robinson, N. I., and Simmons, C. T.: Salinity dynamics of discharge lakes
1113 in dune environments: Conceptual model, *Water Resour Res*, 46, 2010.

1114 Zongxing, L., Qi, F., Wei, L., Tingting, W., Xiaoyan, G., Zongjie, L., Yan, G., Yanhui, P.,
1115 Rui, G., and Bing, J.: The stable isotope evolution in Shiyi glacier system during the
1116 ablation period in the north of Tibetan Plateau, China, *Quatern Int*, 380, 262-271,
1117 2015.

1118

1119 **Figure captions**

1120

1121 **Figure 1** The geological and topographic map of the Yellow River Source Region,
1122 Nianbaoyeze glacial mountains (a), and the sampling settings of the Ximen Co Lake
1123 (b), with the bathymetry map of the lake (d). (c) Photograph of the Ximen Co Lake
1124 and the surrounding geomorphic settings looking northeast direction on 22 Aug 2015,
1125 showing the late-laying snowpack in the U-shaped valleys of the north part of
1126 Nianbaoyeze MT.

1127

1128 **Figure 2** The climatological parameters (wind speed, air temperature, and
1129 precipitation) in the Aug, 2015 recorded from Jiuzhi weather station.

1130

1131 **Figure 3** The temporal distributions of ^{222}Rn (a), water temperature (b), water level
1132 fluctuation recorded by the divers (c), and hourly wind speed and air temperature
1133 recorded in Jiuzhi weather station (d).

1134

1135 **Figure 4** The cross plots of Cl^- versus Na^+ (a), SO_4^{2-} versus Cl^- (b), Ca^{2+} versus Cl^-
1136 (c); The relations of ^2H versus ^{18}O (d), Cl^- versus ^2H (e), and Cl^- versus ^{18}O (f).

1137

1138 **Figure 5** Cross plots of ^{222}Rn versus DIN (a) and DIP (b).

1139

1140 **Figure 6** The conceptual model of ^{222}Rn transient model (a), and three endmember
1141 model (b).

1142

1143 **Figure 7** The results of the final LGD derived from ^{222}Rn transient model.

1144

1145 **Figure 8** The hydrologic partition of the proglacial lake of Ximen CO (a), and the
1146 budgets of DIN (b) and DIP (c).

1147

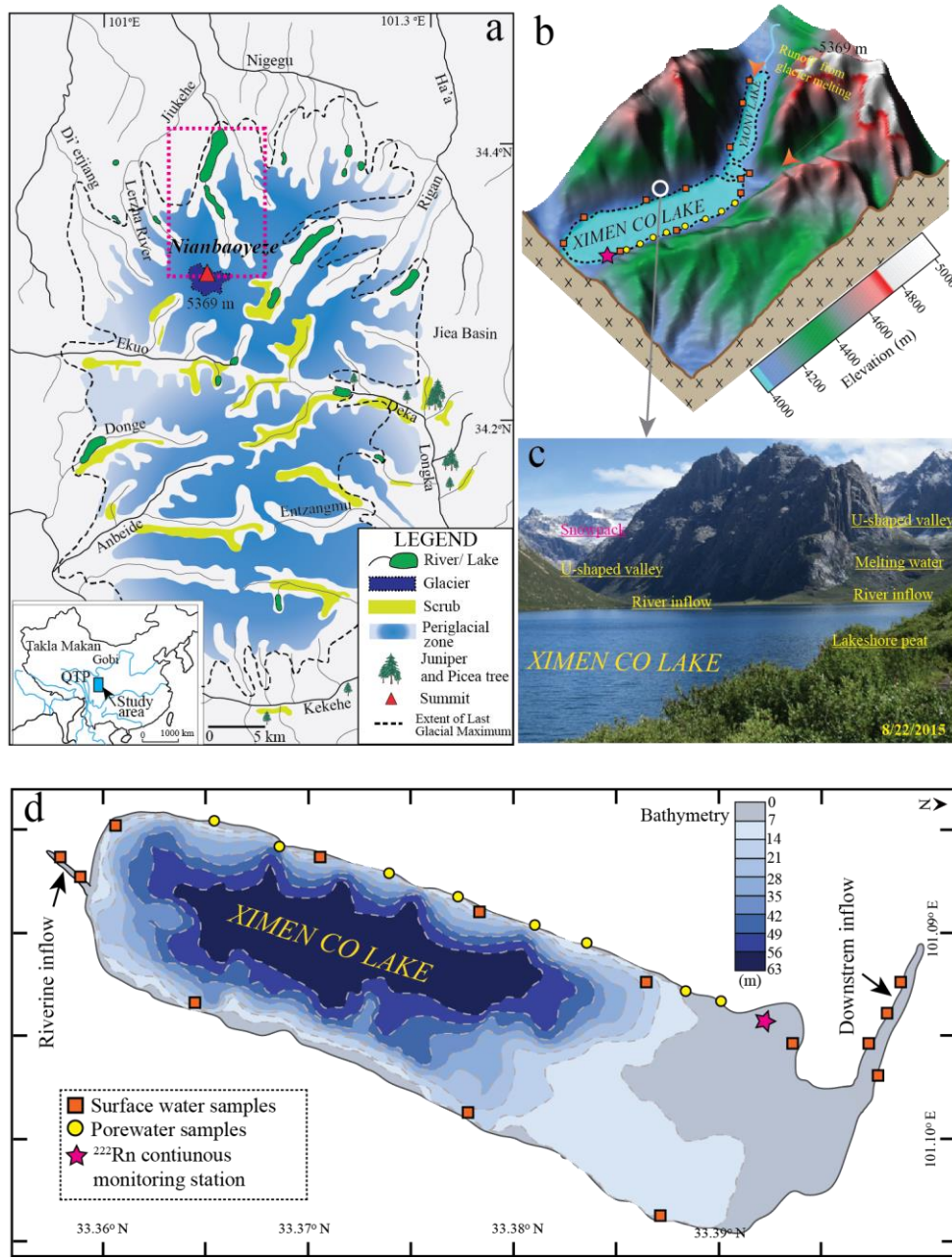
1148

1149

1150

1151

1152 Figure 1



1153

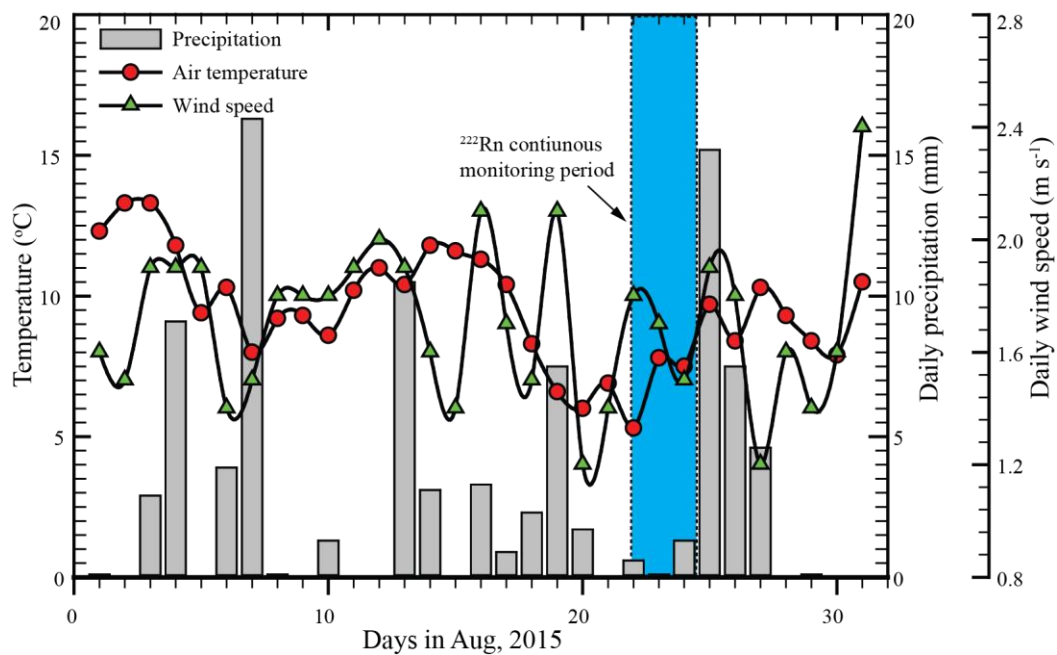
1154

1155

1156

1157

1158 Figure 2



1159

1160

1161

1162

1163

1164

1165

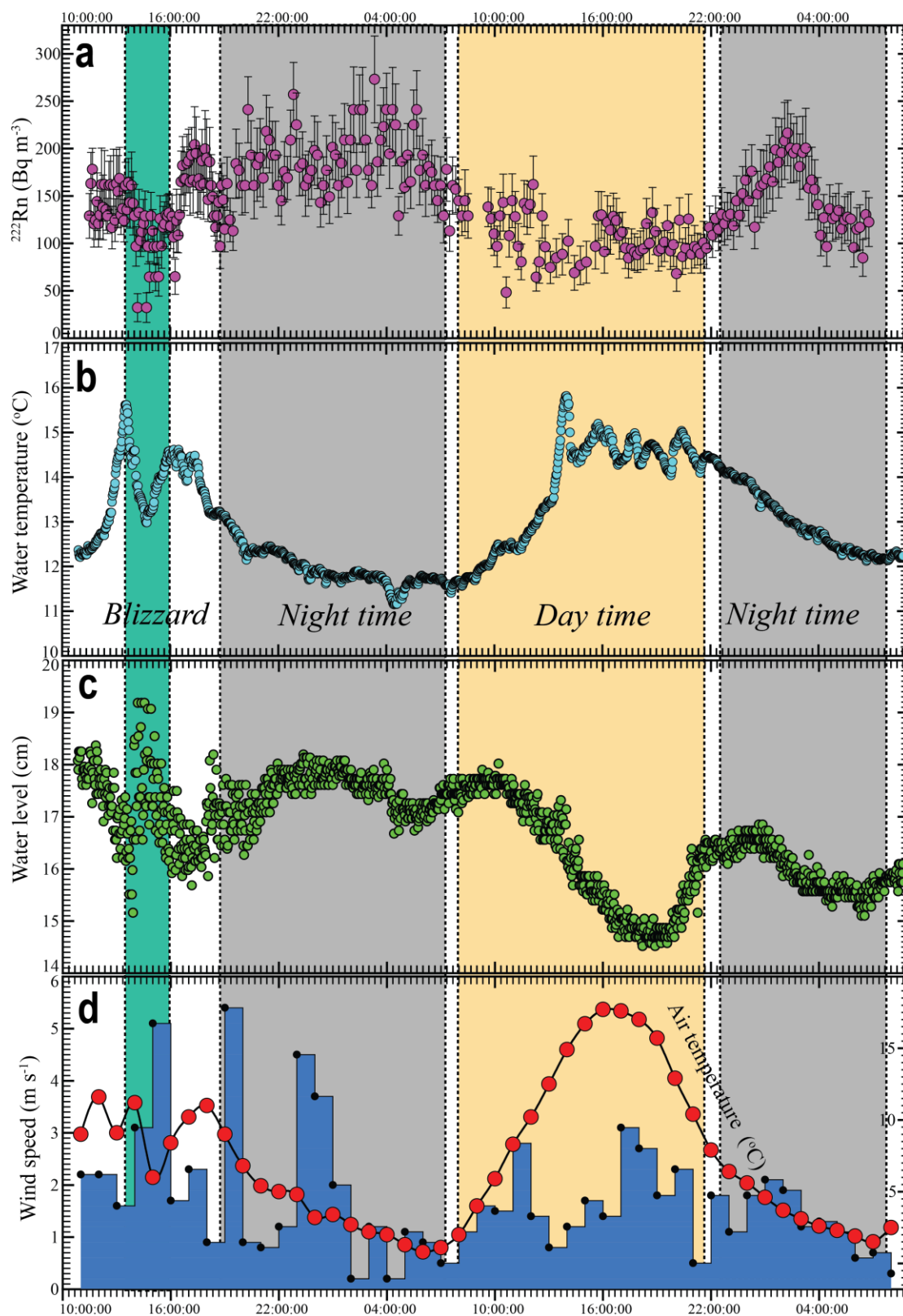
1166

1167

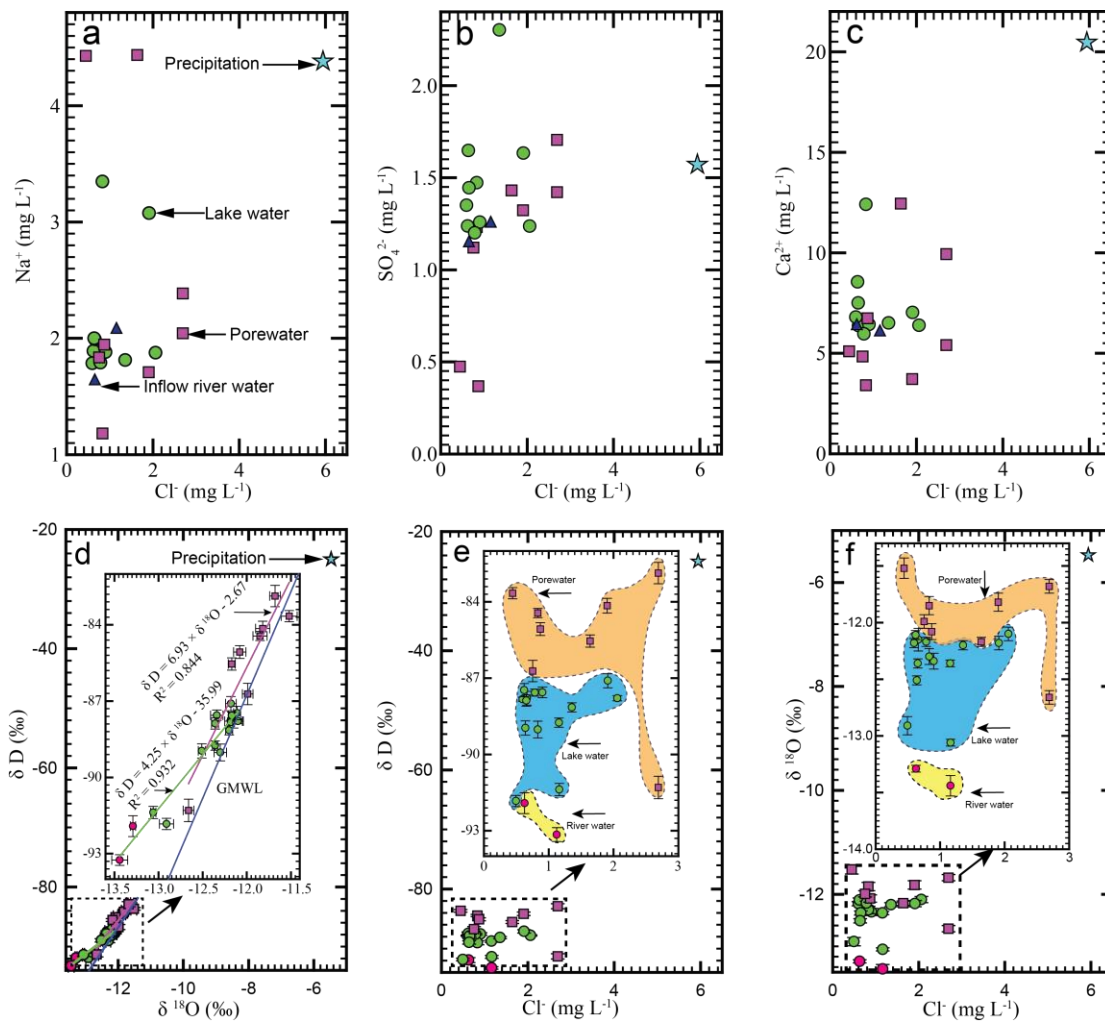
1168

1169

1170



1174 Figure 4



1175

1176

1177

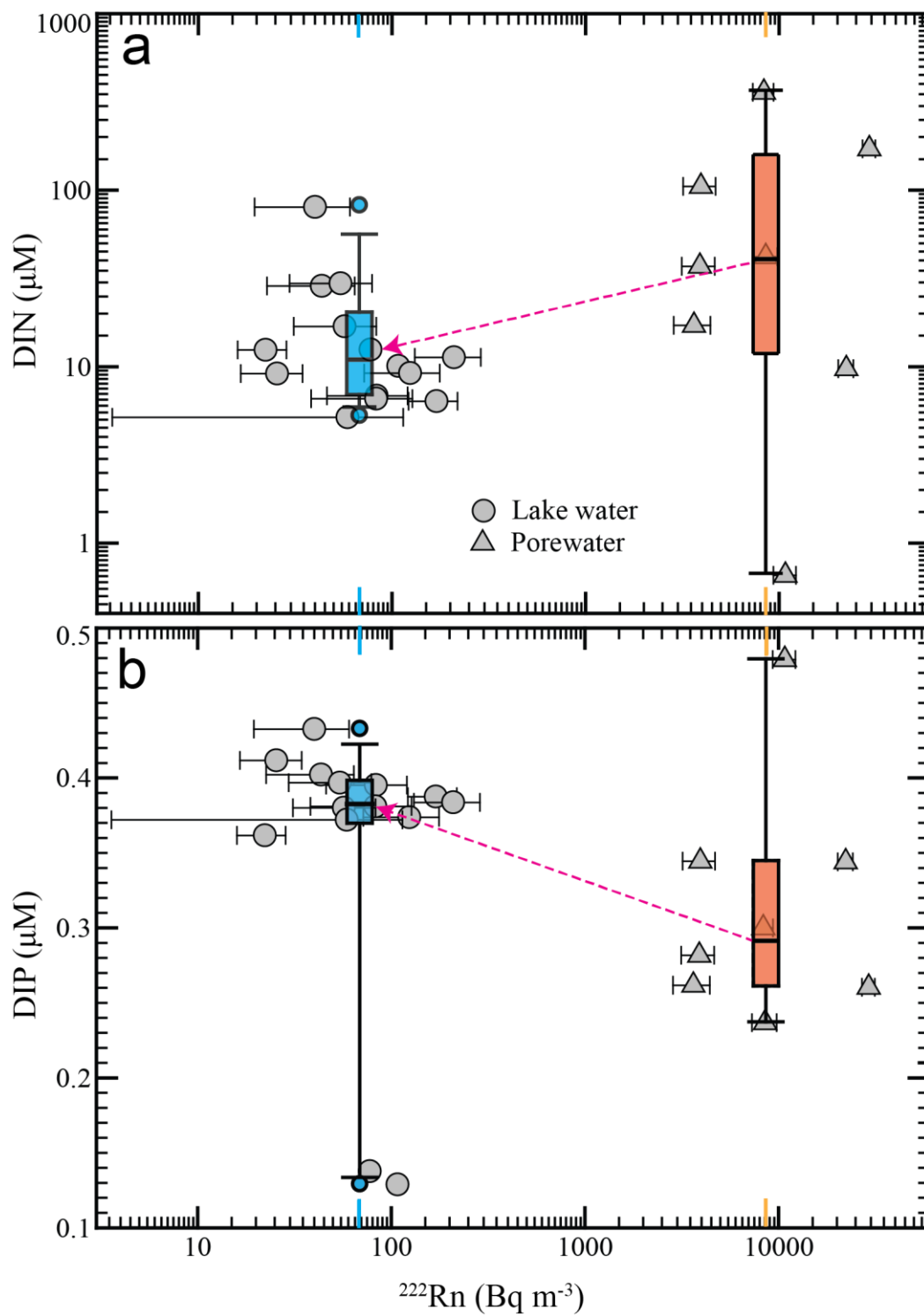
1178

1179

1180

1181

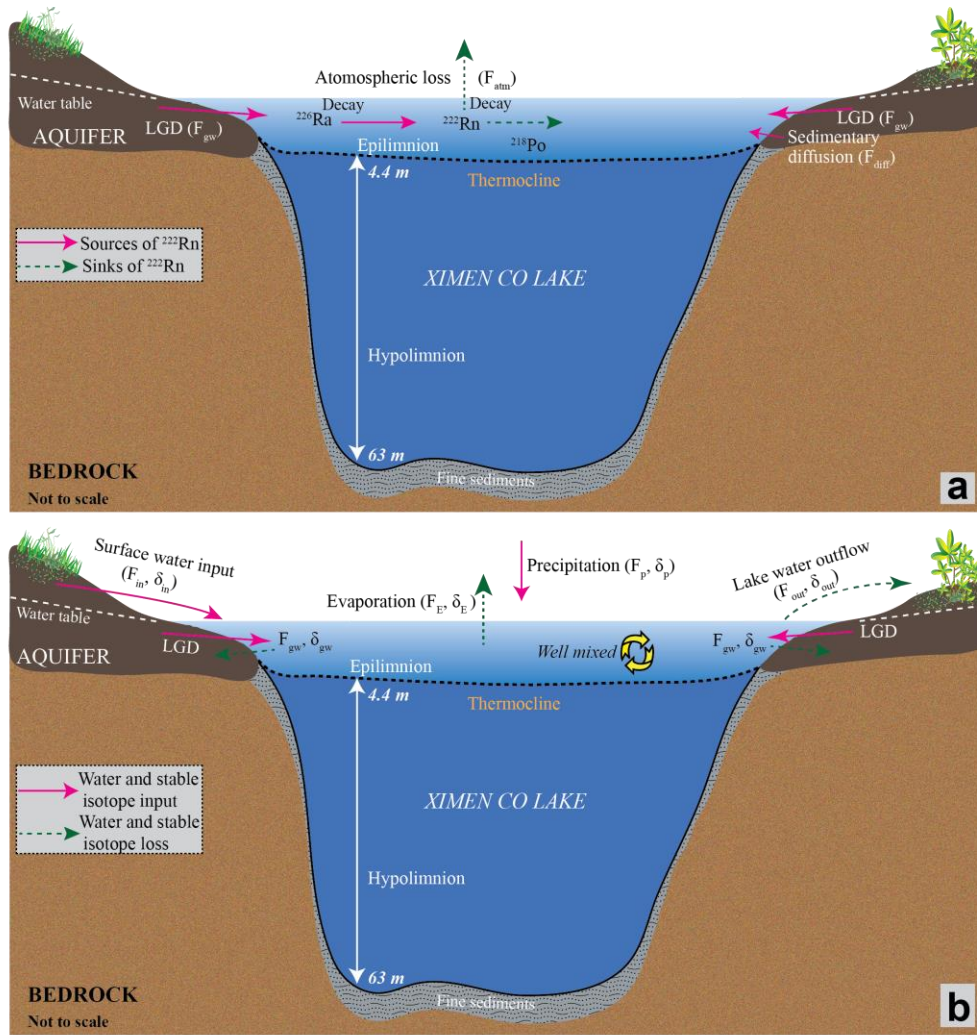
1182



1184

1185

1186



1188

1189

1190

1191

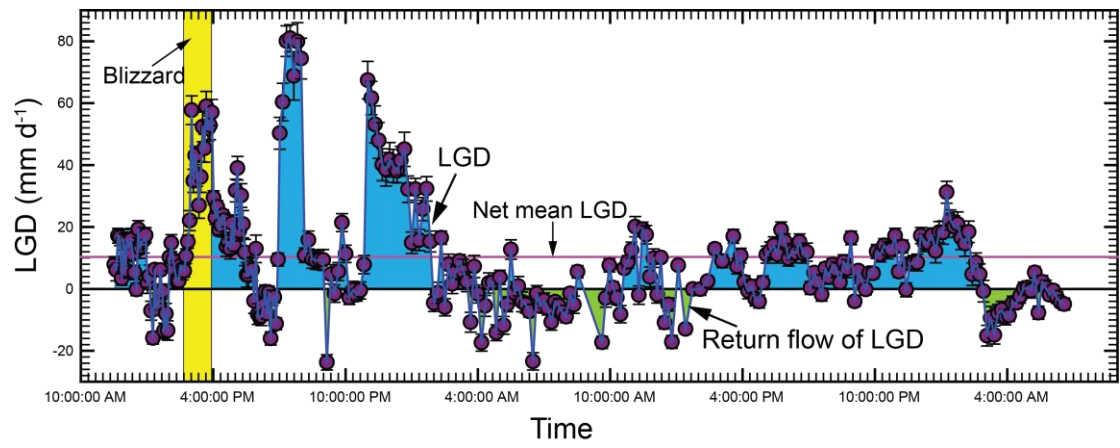
1192

1193

1194

1195

1196 Figure 7



1197

1198

1199

1200

1201

1202

1203

1204

1205

1206

1207

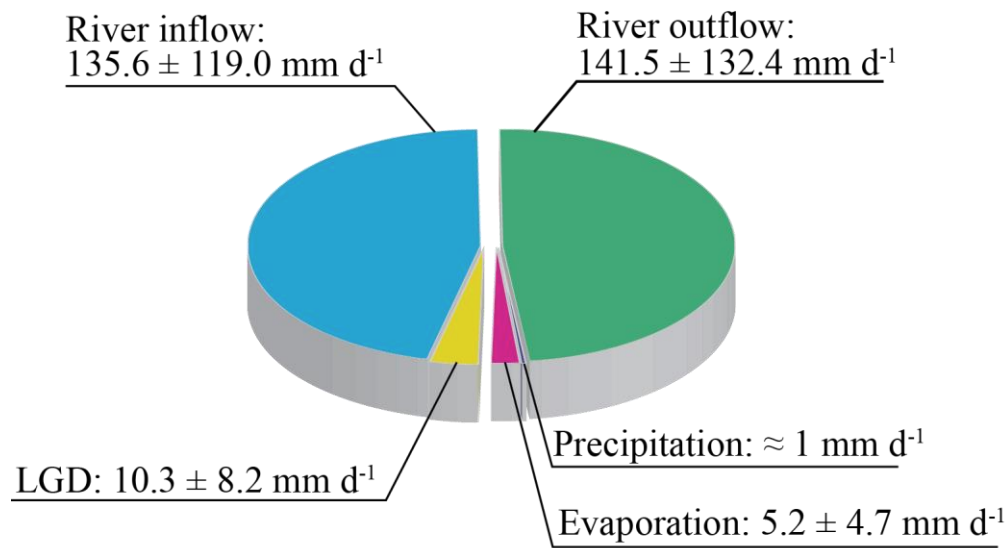
1208

1209

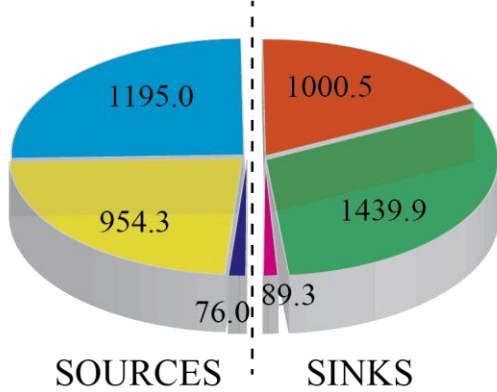
1210

1211 Figure 8

a Hydrologic partitioning



b DIN ($\mu\text{mol m}^{-2} \text{d}^{-1}$)



c DIP ($\mu\text{mol m}^{-2} \text{d}^{-1}$)

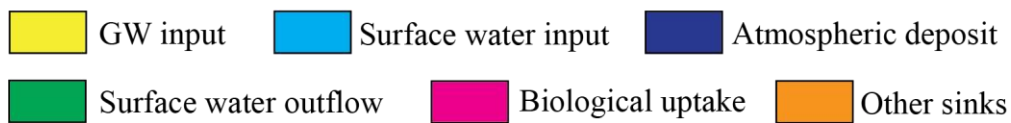
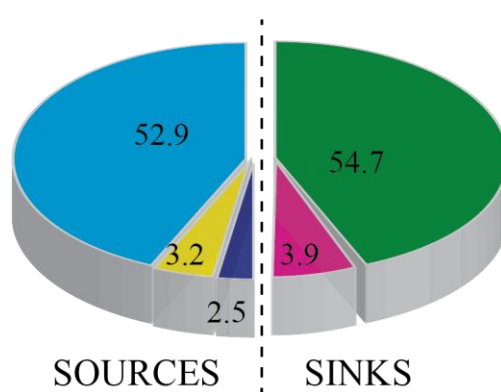


Table 1 Parameters used to establish the mass balance model of ^{222}Rn in Ximen Co Lake.

Parameters	Units or values	Estimated Uncertainty (%)	Evaluation
Wind speed (ω_{10})	0.2 - 5.4 m s ⁻¹	n.a	From Jiuzhi weather stations
Water-air temperature	11.2 - 15.6 °C	n.a	Recorded with probe in the chamber; sensitive to temperature results
Molecular diffusion of ^{222}Rn in water (D_m)	9.2×10^{-6} - 1.0×10^{-5} cm ² s ⁻¹	n.a	1.16×10^{-6} at 20 °C; adjustable for temperature
Molecular diffusion of ^{222}Rn in sediments (D_s)	2.2×10^{-6} - 2.5×10^{-5} cm ² s ⁻¹	n.a	Adjusted for temperature, sediment porosity
Dynamic viscosity (μ)	1.1×10^{-3} - 1.3×10^{-3} cm ² s ⁻¹	n.a	Calculated based on water temperature, density and salinity
Schmidt number (S_c)	1078.6 - 1371.6 [-]	n.a	Calculated as the ratio of ν to D_m
Water depth (H)	4.4 m	n.a	Epilimnion depth of Ximen Co Lake
Decay constant ^{222}Rn (λ_{222})	0.186 d ⁻¹	n.a	Constant
Groundwater endmember ^{222}Rn (C_{gw})	11200 ± 1200 Bq m ⁻³	8 site dependent for Ximen Co Lake	Measured; final result for water flux inversely proportional to ^{222}Rn groundwater concentration
Lake water endmember ^{222}Rn (C_l)	21.6- 418.8 Bq m ⁻³	15-25%	Measured with RAD 7 AQUA
Ambient air ^{222}Rn (C_{air})	1.51 ± 0.97 Bq m ⁻³	15-25 %	Measured with RAD 7 under open loop conditions
Atmospheric ^{222}Rn (C_a)	1.5 ± 1.0 Bq m ⁻³	20-25%	Measured or assumed value, model not sensitive to radon in air variation
$K_{\text{air/water}}$	0.29 - 0.33 [-]	n.a	Calculated based on temperature in the chamber and salinity in lake water
Porosity n	0.31	n.a	Assumed based on literatures
Tortuosity θ	2.05	n.a	Calculated based on porosity
Piston velocity (κ)	0.004 - 1.11 m d ⁻¹	20-25%	Calculated from Equation 3 in supplementary information
^{226}Ra concentration in lake waters (C_{226Ra})	0.01 Bq m ⁻³	≈10%	Measured with RAD7
Diffusive flux of ^{222}Rn (F_{diff})	0.68 - 213.5 Bq m ⁻² d ⁻¹	n.a	Calculated from Equation 9 in supplementary information
Atmospheric flux of ^{222}Rn (F_{atm})	0.7 - 213.5 Bq m ⁻² d ⁻¹	n.a	Calculated from Equation 1 in supplementary information
Groundwater flux of ^{222}Rn (F_{gw})	14.7 - 349.8 Bq m ⁻² d ⁻¹	n.a	Calculated from Equation 1
Inventory of ^{222}Rn (I)	Bq m ⁻²	n.a	Measured with RAD7 AQUA
Groundwater discharge (Q_{gw})	10.3 ± 8.2 (3.5-38.6) mm d ⁻¹	n.a	Calculated from Equation 1

Table 2 Input parameters for the three endmember model of Ximen Co Lake

Input parameter	Description	Values (using ^{18}O as a tracer)	Parametric sources
h	Relatively humidity	0.63	Measured by the humidity meter
T ($^{\circ}\text{C}$)	Water temperature	15.66	Monitored with divers
δ_{surface} (^{18}O) ‰	Surface water isotopic compositions	-12.45	Average value of surface inflow samples
δ_{gw} (^{18}O) ‰	Groundwater isotopic compositions	-11.97	Average value of porewater samples
δ_L (^{18}O) ‰	Lake water isotopic compositions	-12.54	Average value of Ximen Co Lake water samples
F_{gw} (mm/d)	LGD rates	14.18	Calculated based on ^{222}Rn mass balance model
ε^* (^{18}O) ‰	Effective equilibrium isotopic enrichment factor	10.12	Equations 13-14 in supplementary information
C_k (^{18}O) ‰	Kinetic constant for ^{18}O	14.2	Constants based on evaporating experiment
ε_k (^{18}O) ‰	Kinetic enrichment factor	5.2	From Equation 15 in supplementary information
ε (^{18}O) ‰	Total isotopic enrichment factor	15.33	The sum of ε^* and C_k
α^* (^{18}O) ‰	Effective isotopic equilibrium factor	1.01	$\alpha^*=1+\varepsilon^*$
δ_a (^{18}O) ‰	Isotopic composition of ambient air	-23.12	Estimated with δ_{in} and δ_a
δ_{in} (^{18}O) ‰	Isotopic composition of surface inflow water	-13.41	Average value of surface inflow water
δ_E (^{18}O) ‰	Isotopic compositions of evaporating vapor	-35.1	From Equation 12 in supplementary information
$[Cl]_{\text{in}}$ (mgL^{-1})	Chloride concentrations in surface inflow water	0.91	Filed data
$[Cl]_L$ (mgL^{-1})	Chloride concentrations in lake water	1.02	Filed data
$[Cl]_{\text{gw}}$ (mgL^{-1})	Chloride concentrations in groundwater	1.48	Filed data